Review

Vipin Soni, Varun Goel, Paramvir Singh and Alok Garg*

Abatement of formaldehyde with photocatalytic and catalytic oxidation: a review

https://doi.org/10.1515/ijcre-2020-0003
Received January 4, 2020; accepted November 12, 2020;
published online December 14, 2020

Abstract: Formaldehyde is one of the vital chemicals produced by industries, transports, and domestic products. Formaldehyde emissions adversely affect human health and it is well known for causing irritation and nasal tumors. The major aim of the modern indoor formaldehyde control study is in view of energy capacity, product selectivity, security, and durability for efficient removal of formaldehyde. The two important methods to control this harmful chemical in the indoor environments are photocatalytic oxidation and catalytic oxidation with noble metals and transition metal oxides. By harmonizing different traditional photocatalytic and catalytic oxidation technologies that have been evolved already, here we give a review of previously developed efforts to degrade indoor formaldehyde. The major concern in this article is based on getting the degradation of formaldehyde at ambient temperature. In this article, different aspects of these two methods with their merits and demerits are discussed. The possible effects of operating parameters like preparation methods, support, the effect of light intensity in photocatalytic oxidation, relative humidity, etc. have been discussed comprehensively.

Keywords: catalytic oxidation; degradation; formaldehyde; photocatalyst.

Nomenclature

E_a	Activation energy
CO_2	Carbon dioxide
CD	Colloidal deposition
CP	Colloidal precipitation
DRIFTS	Diffused Fourier transform infrared spectroscopy spectra
DOM	Dimensionally order microporous
ev	Electron volt
E–R	Eley–Rideal
FBR	Fixed bed reactor
GHSV	Gas hourly space velocity
IMP	Impregnation
ID	Inner diameter
L–H	Langmuir–Hinshelwood
LSP	Long six pyramids
MVK	Mars–Van krevelan
OMS	Octahedral molecule sieve
PM	Particulate matter
ppm	Parts per million
PCO	Photocatalytic oxidation
RH	Relative humidity
SEM	Scanning electron microscopy
SSP	Short six pyramids
SBS	Sick building syndrome
SP	Six prism
TEM	Transmission electron microscopy
VOC	Volatile organic compound
vol	Volume
λ	Wavelength

1 Introduction

Most of the people spend their time at shopping center, home, car and office, etc. Sometimes, there are more pollution levels indoors compared to outdoors. The common indoor air pollutants are volatile organic compounds (VOCs), carbon oxides (CO and CO_2), nitrogen oxides (NO_x), and particulate matter etc. The possible ways of emission of VOC are from chemical industrial plants, transportation, painting, electroplating, etc. (Wang, Ang, and Tade 2007). There are several origins inside the indoor which contaminate the air. Due to the adverse effect of these contaminants a term "Sick building syndrome (SBS)" has used for the buildings. Filtration and proper ventilation are commonly used for the purpose of the solution to indoor air pollutants as per the typical technology. But hazardous effects arise due to the microbiological and VOC contamination of air (Goswami 1999a).

***Corresponding author: Alok Garg**, Department of Chemical Engineering, National Institute of Technology, Hamirpur, H.P. 177005, India, E-mail: alok.garg.chem@gmail.com
Vipin Soni and Varun Goel, Department of Mechanical Engineering, National Institute of Technology, Hamirpur, H.P. 177005, India
Paramvir Singh, Combustion Research Laboratory, Aerospace Engineering Department, Indian Institute of Technology Bombay, Mumbai 400076, India

So, for restraining pollution inside the building, several techniques have used like air exchange rate and the recent one is by using air purifiers. These air purifiers generally use the filters to remove the particulate matters or sorption material to adsorb odors or gases. But these techniques are not much efficient because they can't eliminate them completely (Zhao and Yang 2003). VOCs e.g. benzene, formaldehyde (HCHO), xylene, and toluene are always discharged in both outdoor and indoor environments through various methods. Long-time divestment to contaminated surroundings though having a very few ppm of VOCs may source of long term sicknesses (Tang et al. 2006a). As per the various health agencies, VOCs are measured as a carcinogenic chemical for human being and longtime contact leads to diseases such as asthma and caused decrement in functioning of pulmonary part. Also, long time expose to formaldehyde can leads to nasopharyngeal cancer.

These VOCs have a very close relationship with sick building syndrome which is an important term used by occupants to represent reduced comfort or health. Fresh painting indoor may produce diseases like asthma (Norbäck, Edling, and Wieslander 1994). A little amount of HCHO can be hazardous to human being in case of long term aspects which produces serious health problems like nasal tumors, skin irritation, mucous membranes irritation of eyes etc. (Li et al. 2016a). In addition, the release of VOCs to the environment can form ozone layer depletion, urban smog in the greenhouse effect and the stratosphere (Liang, Li, and Jin 2012). The cumulative investigation is needed to overwhelmed hazards by VOCs to human healthiness and our environment has caused fast appreciation of toxic aspects of VOCs throughout the past two decades (Goode 1985). It is significant to change injurious volatile organic compounds (VOCs) into the environment-sociable compounds. Various methods have been proposed for reduction of VOCs like physical adsorption (Domingo-Garcia et al. 1999; Matsuo et al. 2008), plasma technology (Liang et al. 2010), plant absorption (Xu et al. 2010; Terelak et al. 2005), photocatalysis (Akbarzadeh et al. 2010; Fu, Zhang, and Li 2011; Li et al. 2010; Photong and Boonamnuayvitaya 2009), and catalytic oxidation (Hu et al. 2015; Sekine 2002; Tang et al. 2006b).

Inside airstream can contain other hazardous contamination like microorganisms (Goswami 1999a). A combination of electrostatic precipitation and photocatalytic oxidation (PCO) has been found as an interactive effect to destroy contamination of air by the microorganism. Removal of microorganism can be done through the electrostatic precipitation. It brings microorganism on the surface coated with photocatalyst (Goswami 1999b). Unlike many other contaminants in indoors which can satisfactorily have diminished by many processes applied, formaldehyde can't be correctly measured just due to its higher vapor pressure i.e. 3883 mm Hg at room temperature i.e. 25 °C and relatively very low boiling point temperature i.e. –19.3 °C (Pei and Zhang 2011). Subsequently catalytic oxidation process needed decreased temperature for degradation of HCHO, the current investigation is grounded on a catalyst for the complete oxidation at environmental conditions. The possible main sources of HCHO emissions are industries, building materials, and transportation (vehicles running by mainly diesel engine) (Singh and Chauhan 2016). Conventional methods, like using filters to remove the contaminants or by sorption materials (like granular activated carbon) to absorb various VOCs are the methods that can only decrease concentration of contaminants in environments. These methods can only alter the stage of the contaminants relatively than the removing them entirely. For HCHO degradation various methods have been reported including (a) chemisorption (b) biological/botanical filtration (c) thermal and non-thermal catalytic oxidation, (d) plasma decomposition with or without using catalyst, and (e) photocatalytic oxidation (PCO).

Plasma cluster ions generated by plasma disintegration process also has the capacity to degrade the HCHO. Generation of plasma is simply through electronic and photoionization the targeting factor through plasma process are density of ion, processing timing, and arrangement of chemicals (Ding et al. 2006). Byproducts and small amount of HCHO are the restriction of plasma technology. Plasma catalyst degradation of HCHO is sometimes problematic due to over formation of ozone (Yuan et al. 2020). In current time botanical filtration is also investigated for degradation of HCHO (Wu et al. 2003). For adsorption of HCHO, biomass bricks are also analyzed and have given an alternate option for diminishment (Zhang et al. 2019). Modified photocatalytic oxidation (PCO) is also a good removal technique for HCHO. Traditional UV light has replaced by visible light in latest PCO for the diminishing HCHO. For diminishment of HCHO, the most suitable photocatalyst TiO_2 with varying absorption of noble metal (Pt, Au, Pd, Ag, etc.) and oxides of transition metal are generally used. Zhu and Wu (2015) has used Pt/TiO_2 photocatalyst for abatement of HCHO.

In this review, there is a thorough description of the photocatalytic oxidation and thermal and non-thermal catalytic oxidation for the degradation of HCHO due to their merits among all mentioned process.

2 Photocatalytic oxidation process

A typical PCO process consists of light energy companionship of water vapor. Water vapors are used for production of

necessary hydroxyl radicals to diminish the VOCs and microbes (Goswami 2003). Water vapour and carbon dioxide (CO_2) are the harmless byproducts of degradation of VOCs using PCO process with semiconductor (Tompkins 2001). The aforementioned ability of PCO attained focus which generally destroys the hydrocarbons with the use of TiO_2 photocatalyst. For regulation of CO_2 i.e., regulated emission there is a carbon dioxide cycle available in nature to balance the concentration of CO_2 in the environment but for the VOCs, there is no such cycle available (Singh and Chauhan 2016). A patent has been filed for disinfecting the indoor air from the clothes, curtain, coverings, etc. and used it for producing the pure air of heating, ventilating, and air conditioning systems (Goswami 2008).

This invention is based on the PCO process in that it uses lightening the surface of photocatalyst with the origin of photons. The photocatalytic oxidation process combines water, oxygen, and VOCs on the catalyst surface to produce H_2O and CO_2 under light radiation. Researchers have used nano Titania (TiO_2) widely as a catalyst which is activated by light energy. Titania has been proven as effective photocatalyst. Photocatalysis technology using TiO_2 has sufficient potential for the purification of organic pollutants and wastewater (Hashimoto, Irie, and Fujishima 2005; Hoffmann et al. 1995; Wu et al. 2003). There are further several photocatalysts which have been used for degradation of HCHO which are ZnO, Al_2O_3, ZrO_2, WO_3, SnO_2, CeO_2, ZnS, Fe_2O_3 and CdS (Hoffmann et al. 1995). But the most popular photocatalyst used for oxidation of formaldehyde into harmless gases is TiO_2 and ZnO. TiO_2 is the readily available, relatively inexpensive, chemically stable element. Holes generated by photo-oxidation process are highly oxidizing in nature (Jin et al. 2007).

Fe_2O_3–TiO_2 supported with Pt doping is also an excellent catalyst for the decomposition of formaldehyde (Yang et al. 2000). TiO_2 doped with Ag metal also shows enhanced photocatalytic activity for the devastation of bacterial spores as a comparison to typical photocatalysis (Vohra et al. 2005). Arranging the photocatalysts into the active catalysts between Ti, Zn, and tungsten; the result shows that: TiO_2 (anatase) < ZnO < WO_3. There is generally two crystal form of TiO_2 available: anatase and rutile. The difference between these two structures is of band gaps. The band gaps of anatase and rutile phases are 3.23 and 3.02 ev respectively.

2.1 Working principle

When TiO_2 is irradiated by light, electron and hole pairs are generated in the bulk particle. While producing holes, electrons gain energy to leave from valence band to conduction band with crossing the band gap. The holes in valence band have great oxidative power and due to this, it makes hydroxyl radicals with reaction of absorbed hydroxide ions. This formation process is accountable for photo oxidation of HCHO. But alone TiO_2 has the restriction in case of application because of requirement of UV light and lesser solar radiation coming to Earth surface. Although this restriction has been eliminated by expansion of optical retaliation of TiO_2 up to visible light from UV. These UV lights are harmful to the human body. Decomposition through irradiation of light on catalyst surface is shown in Figure 1.

Electrons and holes permit oxidation and reduction on the photocatalyst surface (Ohtani 2008). The corresponding equation of generation of holes and electron due to irradiation of photon can be written as:

$$TiO_2 + \text{photons} \rightarrow \text{electron}\,(e^-) + \text{hole}\,(h^+) \qquad (1)$$

In above reaction process, holes are responsible for oxidation process while electrons for reduction which is also shown in Figure 2.

$$\text{Oxidation reaction}: \text{hole}\,(h^+) + OH^- \rightarrow OH^* \qquad (2)$$

$$\text{Reduction reaction}: e^- + O_{2ads} \rightarrow O_{2ads}- \qquad (3)$$

The role of hydroxyl radical (OH*) is important as formaldehyde gas is passed through the photocatalytic oxidation device, it oxidizes the gaseous HCHO into harmless CO_2 and H_2O. These hydroxyl radical generally derived from oxidation of water vapor or adsorbed hydroxyl anion.

Different activity during the PCO has various advantages (Ollis 2000);

- It is recognized as the safe process which commonly uses the anatase TiO_2 as a photocatalyst, an *n*-type semiconductor found also in some toothpaste and pharmaceutical suspensions.
- During the oxidation process, final source of oxygen is molecular oxygen which is a safer oxidant as compared to hydrogen peroxide or ozone etc.

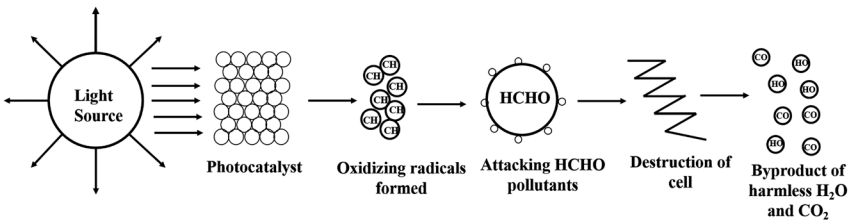

Figure 1: Formaldehyde degradation due to irradiation of light on catalyst surface.

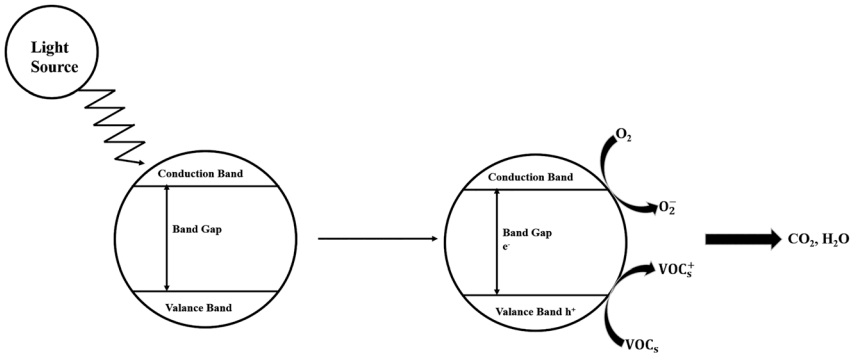

Figure 2: Process of generation of electron and holes in conduction and valence band.

- The photocatalysis process generally requires room temperature.
- As mentioned above hydroxyl radicals are photo-generated in the surface of Titania which is simpler process since there are many mechanisms available for the oxidation process.

UV–Vis light is responsible for the creation of electron–holes pairs in the photocatalyst during PCO of VOCs.

2.1.1 UV responsive photocatalysts

Emphasize on different types of defects in TiO_2 like surface oxygen vacancies, Ti interstitials and oxygen atoms for high impact on the photo-dissociation of HCHO. These defects have a high impact on the thermal excitation of oxygenated organic compounds on TiO_2 (Benz et al. 2009; Bowker and Bennett 2009; Landis et al. 2012; Li and Diebold 2009; Lu, Linsebigler, and Yates 1994; Wang et al. 2003; Zhang et al. 2007). Due to wide energy bandgap titanium oxide activates only through ultraviolet (UV) region. TiO_2 is activated through the irradiation of photon ($h\nu$) on the surface with ultra-band energy from the UV light source. Formation of electrons and holes caused oxidation of absorbed toxic organic pollutants and form CO_2 and H_2O (Zou et al. 2006). All the literature tills now had shown that the surface of noble metal sides has the most active site for the oxidation process of HCHO (Kecskés, Raskó, and Kiss 2004). In different semiconductor materials, ZnO has bandgap relatively equal to TiO_2 (Xu and Schoonen 2000) and the origin of ZnO is quite wide. But UV activation of ZnO was not easy till suitable morphological differences invented. It is quite understood that defects influenced the photocatalysis (Gupta, Barick, and Bahadur 2011; Shi et al. 2011). Therefore, by improving the morphologies and the defects in ZnO enhance the photocatalytic properties. UV activation of ZnO enhances by etching the sample with Argon (Ar) (Liao et al. 2013). The 254 nm wavelength UV lamp emitted higher photons which have contributed efficient degradation of HCHO over TiO_2/UV. Doping of silver (Ag) or cerium (Ce) ions could enhance photocatalytic property of TiO_2. The degradation of HCHO over Ce-TiO_2, Ag-TiO_2, and TiO_2 can be arranged in order of Ce-TiO_2 > Ag-TiO_2 > TiO_2 (Liang, Li, and Jin 2012). The reason for increasing photocatalytic oxidation due to doping is increase of chemisorbed oxygen at the surface of TiO_2 (Yang et al. 2006). It creates an imbalance charge vacancy on the catalyst surface.

2.1.2 Visible light responsive photocatalysts

Since UV sources are power consuming, costly, and hazardous to health, visible sources are readily available, inexpensive and energy saving. To enhance the spectrum, range of photocatalyst from UV light to visible light; three methods have been used: transition metal doping into TiO_2; doping of nitrogen into TiO_2 and with sensitizing dyes. Transition metal ions like Mn, Fe, V, Cr, Co, Ni or Cu increases the spectrum region into the visible light region (Zang et al. 2000). Presence of metals like Li^+, Ce^{3+}, Co^{3+}, Zn^{2+}, Cd^{2+}, Cr^{3+}, Fe^{3+}, Al^{3+}, Mn^{2+}, and Pt sufficiently change the photocatalytic activity of TiO_2. Different nitrogen-doped TiO_2 were used as photodegradation of gaseous HCHO (Zang et al. 2000). In the case of visible light irradiation $TiO_{2-X}N_X$ has better photocatalytic activity than TiO_2. The addition of ZrO_2 into$TiO_{2-X}N_X$ possesses higher porosity, higher surface area, and enhanced thermal stability rather than $TiO_{2-X}N_X$ samples (Wang et al. 2006).

A very few literatures have quoted the effect of noble metal on photocatalyst. Noble metal doping into TiO_2 has a higher capability to transfer electrons. In the case of Pt-TiO_2, Pt plays the role of core of core–shell Pt-TiO_2 which can increase the photo-activity for abatement of HCHO (Zhu and Wu 2015). To enhance the spectrum, range of photocatalyst from UV to visible range, gold (Au)

nanoparticle support was used on TiO_2 because of its high visible light absorption (Tsukamoto et al. 2012; Wang and Astruc 2014; Yang et al. 2014). The preparation of Au nanocatalyst affects the catalytic activity process. Atmospheric pressure oxygen has strong activity for CO oxidation which activates the Au/TiO_2 nanocatalyst (Zhang et al. 2015a).

There is some literature available on silver ion (Ag^+) (Liu et al. 2003; Venkataraj et al. 2002) which suppressed the recombination of charge at the surface of TiO_2. Doping of silver into TiO_2 reduces the anatase growth rate which ultimately results in low crystallinity of anatase structure with comparison to pure TiO_2, the crystallite size of Ag-doped TiO_2 decreases. TiO_2-Ag and TiO_2-Ag-TEA permit higher degradation rates as compared to pure TiO_2 (Kocareva, Grozdanov, and Pejova 2001). The different state of silver Ag^+, Ag^0, and metal Ag at the surface of TiO_2 suppresses the recombination of electron–hole which leads to an increase the photocatalytic activity of TiO_2 (Ubolchonlakate, Sikong, and Tontai 2010). The mechanism involves;

$$2Ag^+ + HCHO + 3OH^- \rightarrow 2Ag + HCOO^- + 2H_2O \quad (4)$$

HCHO degradation by TiO_2 or TiO_2 composite can be written as:

$$HCHO + OH^* \rightarrow HCO^* + H_2O \quad (5)$$

$$HCO^* + OH^* \rightarrow HCOOH \quad (6)$$

$$HCOOH + 2h^+ \rightarrow CO_2 + 2H^+ \quad (7)$$

Metal and non-metal doping are suitable techniques for improving the photo-activity of Titania. Doping metal atoms depressed the recombination of electrons and holes while doping nonmetal atoms can generally influence the different properties of titania such as lattice structure, band gap (Asahi et al. 2001; Khan, Al-Shahry, and Ingler 2002; Lin et al. 2007; Ohno et al. 2004). Photocatalyst doped with silver ion has been developed by Vohra et al. (2006) to devastate the airborne microbes. The result shows that photocatalyst doped with Ag can be used effectively for high concentrated contaminants. Zhao et al. (2004) have quoted that spectrum region and photocatalytic activity can be improved by doping with non-metal boron and metal oxide Ni_2O_3. Zhang et al. (Liu et al. 2008) have reported that strong absorption in the visible range for nitrogen nickel doped Titania. Absorption line is moved to lower energy region for the different proportion of nitrogen nickel doped titania such as N (0.010) Ni (0.015) TiO_2 (600), while no absorption for samples Ni (0.015) TiO_2(600) and pure TiO_2(600) have observed. The bandgap energies were 2.29, 2.30, 3.17 and 3.15 ev have been reported for sample N (0.010) Ni (0.015) TiO_2 (600), N (0.010) TiO_2 (600), pure TiO_2 (600) and Ni (0.015) TiO_2 (600).

It shows the decrease in the bandgap due to the mixing of nitrogen. Transition metal ions doping in TiO_2 inject high energy ions into the TiO_2 lattice during ion implantation techniques. Anpo, Tanahashi, and Kubokawa (1980), Anpo et al. (1985, 2000), Yamashita et al. (1998) have experimented with the transition metal doping like V, Cr, and Fe on TiO_2. Lam et al. (2007) has reported that in absence of Cr ion; even 1.2 mW/cm^2 visible intensity light could not activate the photo-activity of TiO_2. After injection of Cr ion Cr/TiO_2 thin film gets activated for visible light. Heterostructured combination of waste zeolite and graphitic carbon nitride supported on TiO_2 has prepared by Liu and Lin (2019) under the market available LED light for diminishment of HCHO. The decomposition of formaldehyde in the range of UV and visible light at different wavelengths is given in Table 1.

2.2 Kinetics and mechanism involved

For progression of the photocatalysis, generally initial steps are as below:

$$TiO_2 + h\nu \rightarrow \text{holes} + \text{electrons} \quad (8)$$

$$\text{holes} + OH^- \rightarrow {}^{\bullet}OH \quad (9)$$

$$Ti^{4+} + e^- \rightarrow Ti^{3+} \quad (10)$$

$$Ti^{3+} + O_{2ads} \rightarrow Ti^{4+} + O^-_{2ads} \quad (11)$$

$$OH^{\cdot} + \text{pollutant} \rightarrow \text{oxidized polltant} \quad (12)$$

The absorbed formaldehyde on the surface of catalyst will be oxidized by hydroxyl radicals and superoxide ions which are also termed as highly reactive components. During this process some byproducts would also have formed which will be converted in CO_2 by $O_2^{\bullet}$ or $O^{\bullet}$ oxidation. Photo-degradation process for formaldehyde in the steps of oxidation and reduction can be inscribed as follows (Ding et al. 2006):

$$TiO_2 \rightarrow^{\text{photon}} \text{electrons} + \text{holes} \quad (13)$$

Oxidation

$$HCHO + H_2O + 2h^+ \rightarrow HCOOH + 2H^+ \quad (14)$$

$$HCOOH + 2h^+ \rightarrow CO_2 + 2H^+ \quad (15)$$

$$\text{Reduction } O_2 + 4e^- + 4H^+ \rightarrow H_2O \quad (16)$$

Table 1: Degradation of formaldehyde due to a different wavelength of the light source.

S. no.	Catalysts	Parent material	Inlet condition	Type of reactor	Doping element	Preparation method	Weight (%)	Time (h)						Wavelength (nm)				Result
								1	2	4	6	8	10	250	300	350	400	
1.	Photo catalyst (Anpo et al. 2000)	TiO_2	HCHO-400-ppm, 500 W Xenon Lamp	A cubic, airtight, SS reactor (30 cm × 30 cm)	Ni, N	Sol gel method	N(0.01)[a] Ni(0.015)[b] TiO_2(600)[c]	57.76	85	–	–	–	–	1.75	1.69	1.29	0.21	Addition of Ni and N enhanced catalytic activity to the visible range
							N(0.01)[a] Ni(0.015)[b] TiO_2(700)[c]	54.35	77.27	–	–	–	–					
							N(0.01)[a] Ni(0.015)[b] TiO_2(500)[c]	50.6	74	–	–	–	–					
							N(0.01)[a] TiO_2(600)[c]	34	54.166	–	–	–	–	1.70[d]	1.55[d]	0.77[d]	0.09[d]	
							P25	18	29	–	–	–	–					
							Ni(0.015)[b] TiO_2(600)[c]	4	6.5	–	–	–	–	1.31[d]	1.29[d]	1.14[d]	0.87[d]	
							TiO_2(600)[c]	3	6					1.25[d]	1.21[d]	1.25[d]	0.94[d]	
2.	Photo catalyst (Liang, Li, and Jin 2012)	TiO_2	A lamp (λ = 200–300 nm) with maximum light intensity 254 nm, flow-rate – 3 L/min,	Cylindrical photo-catalytic reactor with inner diameter 18.0 mm	Ce	Sol gel method	5 wt%	70	70.5	75.5	90	95.4	–					Ce–TiO_2 catalyst possesses best oxidation capacity among them under UV region
					Ag		5 wt%	60	61	70	80	92.33	–					
					Pure			50	60	65	75	89.27	–					
3.	Photocatalyst (Liao et al. 2013)	ZnO	100 ppm formaldehyde gas, LED used here were ultraviolet (365 ± 5 nm, 3.6 mW/cm^2) and white (400–800 nm, 35.5 mW/cm^2) light, room temperature (25 °C)	Gas phase photo-catalytic reactor with inner volume of 1.2 L		Metal organic framework with molar ratios of $ZnNO_3$-$6H_2O$/terephthalic acid/DMF/F127/HCl/H_2O/ethanol	SP							1.06	1.43	1.42	0.36	Under white light the oxidizing tendancy of SP-10 h and LSP-10 h is similar to TiO_2
							SP–5h							0.92	1.19	1.23	1.77	
							SP–10 h							0.77	1.09	1.77	0.76	
4.	Photo catalyst (Akbarzadeh et al. 2010)	TiO_2	20 mL of aqueous solution of formaldehyde (200–500 ppm)	Photocatalytic reactor	V_2O_5	Sol–gel	TiO_2	0.22[d]	0.43[d]	0.91[d]						0.49	0.16	Addition of vanadium shifts the band from UV range to visible range
							0.5% V_2O_5	0.61[d]	1.13[d]	2.65[d]								
							1% V_2O_5	0.87[d]	1.65[d]	3.57[d]							0.21	
							2% V_2O_5	1.22[d]	2.28[d]	4.74[d]							0.34	
							4% V_2O_5	1.52[d]	2.69[d]	5.52[d]							0.39	
5.	Photo catalyst (Zhu and Wu 2015)	TiO_2	18 W daylight lamp at room temperature (initial HCHO	Photocatalytic reactor	Pt	Reverse micelle sol–gel method	1 wt%	84.52	84.52	90.48								Band energy shifted from UV to visible light range due to
							1 wt%	91.47	97.62	97.62								

Table 1: (continued)

S. no.	Catalysts	Parent material	Inlet condition	Type of reactor	Doping element	Preparation method	Weight (%)	Time (h)						Wavelength (nm)				Result
								1	2	4	6	8	10	250	300	350	400	
			concentration = 10 ppm)															incorporation of Pt into TiO_2
6.	Photo catalyst (Huang et al. 2013b)	TiO_2	45 W energy saving lamp provided the UV–Vis light source, formaldehyde concentration was 1.0 ± 0.5 mg	Self-designed glass reactor (0.22 m^3, 600 × 600 × 600 mm)	Zr	sol–gel	Reference	1.04[e]	1.04[e]	1.03[e]	1.03[e]	1.03[e]	1.03 [e] 1					The band response of TiO_2 is moved from UV to visible range due to doping of Zr
							5 wt%	1.28[e]	1.00[e]	0.99[e]	0.98[e]	0.97[e]	0.95 [e]					
							8 wt%	1.03[e]	1.02[e]	1.01[e]	0.99[e]	0.97[e]	0.96 [e]					
							10 wt%	1.01[e]	1.00[e]	0.98[e]	0.98[e]	0.96[e]	0.95 [e]					
							12 wt%	1.03[e]	1.03[e]	1.01[e]	1[e]	0.97[e]	0.96 [e]					
							15 wt%	1.01[e]	1.01[e]	1.01[e]	1.01[e]	1.00[e]	0.99 [e]					

a = atomic ratio of N to Ti, b = atomic ratio of Ni to Ti, c = calcination temperature, d = conversion in absorbance unit (a.u.), e = conversion in mg/m^3.

The above reactions illustrated that four h^+ is stoichiometrically required for complete oxidation of one HCHO molecule.

2.3 Kinetic experiments of photocatalytic oxidation

Extracting data from kinetic experiments is the prime factor for the optimum design of the reactor. An ample number of the test has been performed by Goswami, Trivedi, and Block (1997) by changing the influencing parameters like water vapor content, the intensity of light, air velocity, etc. over the TiO_2 photocatalyst for varying the reaction timing for the destruction of contaminants.

2.3.1 Light sources and intensity

In photocatalytic process recombination electron–hole pair and interstitial charge transfers are second-order and first-order processes respectively which show that while increasing the light intensity rate of recombination of electron and holes increases which ultimately lower the quantum efficiency (Yang and Liu 2007). By literature it has been noted that reaction rate is directly proportional to light intensity for the low intensity of light and is however proportional to the square root of intensity of light under medium light intensity and totally independent of light intensity under high light intensity.

2.3.2 Effect of water vapor

Total photocatalytic decomposition of formaldehyde into CO_2 gets decreased due to the insufficient water vapor. 50% relative humidity along with sufficient stay time creates an efficient quantity of water molecules to cause inactivation of microorganisms (Goswami 1998). On the other hand, on surface of catalyst, the presence of excess water vapor can also reduce the reaction rate because excess water vapor can block active sites on the surface. The effect of water vapor on formaldehyde oxidation can analyze as: with an increase of water vapor from low to high, the oxidation rate will also increase proportionally but after that as water vapor will cross the optimum level the reaction rate immediately start decreasing. For the below, 10 ppmv concentration of formaldehyde with relative humidity ranges between 15 and 60% Langmuir–Hinshelwood suggests 1st order oxidation rate for formaldehyde (Zhao and Yang 2003). Up to 35% RH the decomposition of formaldehyde into CO_2 increases after that it will start diminishing hence 35% RH turns to be the optimal condition for degradation rate (Liang, Li, and Jin 2012).

In existence of water vapor, the increased reaction rate is observed due to the behavior of hydroxyl radicals as a hole trap to create surface occupied hydroxyl radicals. During photocatalysis hydroxyl radicals carried out two action, one is capturing of HCHO molecules and the second one is reducing the electron–hole recombination (Liang, Li, and Jin 2012).

2.3.3 Contaminant concentration

The concentration of reactants may also have an impact on the reaction rate similar to light intensity and relative humidity. Different reactant proportion alters the reaction rates. As per Noguchi et al. (1998), HCHO concentration above the 600 ppmv reduces reaction rates. Deng et al. (2017) have also given the range of initial concentration to determine the order of the reaction. According to him HCHO ranging from 35 to 107 ppm does not affect the conversion of formaldehyde. Langmuir–Hinshelwood model directly relates between contaminant concentration and reaction rates. Generally, the actual concentration of VOCs is lesser in normal indoor but for the investigation of the oxidation process, there is a need for higher concentration.

2.3.4 Photocatalytic reactors

Basically the surface of reactors layered with catalyst is used to degrade the VOCs. Flat plate and annular reactor are the basic structure for the evaluation of kinetic models. Other than this, for achieving greater surface area different models are design which ultimately improves performance and provide better radiation on catalyst surface. Commercially available examples are: monolith, packed bed and fluidized bed photo catalytic reactors. With some improvisation for increasing the catalyst area other reactors are corrugated plate (Passalía, Alfano, and Brandi 2012), multi plate, multi annular (Zazueta, Destaillats, and Puma 2013), foam packed bed (Ibhadon et al. 2007) and paper based immobilized TiO_2 reactors (Adjimi et al. 2014).

For greater air inlet, plate type and annular type reactors were not commercially appropriate. Though these types' reactors are only used for investigating different kinetic parameters. For appropriate design and greater conversion over unit mass of catalyst, packed bed reactors are usually available. This reactor also has the limitation of unit maintenance. For overcoming this fluidized bed reactors are the option with low pressure drop. Monolith reactors possess increased flow, low pressure drop and

compact design. This has also limitation of quick diminishment of light intensity. This limitation can overcome with improvisation of optical fibers passing with each monolith (Boyjoo et al. 2017).

To overcome the different drawback of photo catalytic reactors several improvements have been done to increase the efficiency. For example: Qin et al. (2020) has used annular reactor to provide uniform illumination of catalyst and increased flux flow of the contaminants. This modified photocatlytic reactor is widely used in practical use. They have concluded that degradation efficiency of HCHO with foil catalyst annular photo reactor was 2.28 times greater than commercial TiO_2 powder catalysts.

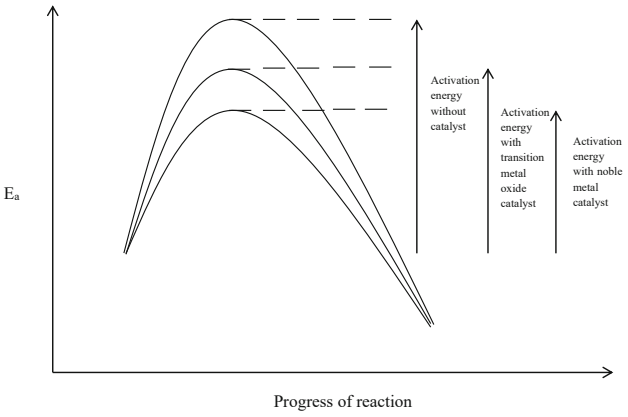

Figure 3: Requirement of energy with different catalyst.

3 Catalytic oxidation

Due to the formation of harmless CO_2 and H_2O through highly effective total degradation of HCHO, photocatalytic oxidation was a demanding option for complete catalytic oxidation of HCHO. Various by-products which are harmful in nature like CO were found in the degradation of HCHO (Yang et al. 2007). Another disadvantage that makes PCO insufficient is that catalytic surface gets deactivated by time. Moreover, a catalyst possesses high reactivity with the confirmation of restricted energy requirement for the process of catalytic oxidation. At an increased temperature i.e. thermal or at room temperature i.e. non-thermal, catalytic oxidation uses a catalyst for diminishment of VOCs. Hence, at ambient temperature catalytic oxidation possess assuring option for diminishment of VOCs emission since it converts VOCs into CO_2 (Zhang, Jiang, and Shangguan 2016). Catalytic oxidation also termed as a low temperature (293–673 K) degradation process and it is termed as powerful post remedial technology.

The major advantage of catalytic oxidation includes the formation of CO_2 and H_2O from HCHO with no intermediate pollutants (Bai, Arandiyan, and Li 2013; Pei and Zhang 2011). General catalysts in catalytic oxidation process increase the chemical reaction by providing sufficient activation energy (E_a) which is shown in Figure 3. Transition metal oxides (Co, Ag, Ni, and Mn) (Chen et al. 2009; Imamura et al. 1994; Ma et al. 2014; Tang et al. 2006b; Wen et al. 2009; Xu et al. 2011) and supported noble metal (Pd, Rh, Pt and Au) (Arzamendi et al. 2009; Huang and Leung 2011a; Imamura et al. 1991; Kim, Park, and Hong 2011; Li et al. 2011; Sekine 2002; Zhang and He 2007; Zhang, He, and Tanaka 2005; Zhang, He, and Tanaka 2006; Zhang et al. 2012) catalysts are the established catalysts for the HCHO degradation at room temperature.

3.1 Noble metal catalysts

For degradation of HCHO, noble metals support effect the catalytic activity strongly. Many researchers have been proposed in support Pt, Pd, Au, Rh which is having strong catalytic activity and stability. Complete oxidation of formaldehyde can be achieved through noble metal. In Figure 1, it has been shown that activation energy requirement after noble support gets decreased and ambient temperature is sufficient for oxidation of HCHO. Among all noble metal catalysts, Pt support affects strongly and it is sufficient to do oxidation at ambient temperature. Generation of CO_2 and H_2O on noble doped supports is shown in Figure 4.

3.1.1 Pt supported noble metal catalyst

Platinum has a very high dispersion degree over TiO_2 (Zhang, He, and Tanaka 2005). Zhang, He, and Tanaka (2005) have reported that Pt/TiO_2 catalyst has a 100% conversion of HCHO. Peng and Wang (2007) has reported that at 20 °C HCHO conversion was only 14.3% but at 120 °C the conversion becomes 97% even at 1% Pt loaded TiO_2. The optimized use of Pt is a great concern till now since it is

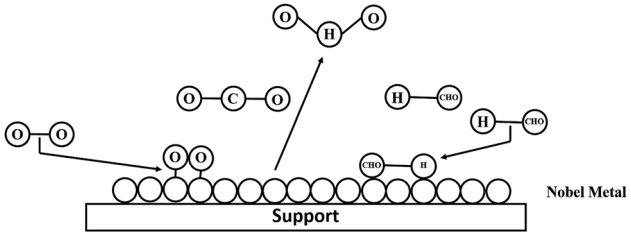

Figure 4: Formaldehyde conversion in CO_2 and H_2O on noble metal doping.

highly expensive from other catalysts. A very low concentration of Pt even at 0.1 wt% at TiO_2 possesses excellent conversion of HCHO at ambient temperature (Huang and Leung 2011b).

A comparative catalytic activity has been shown with taking pure TiO_2 and Pt-TiO_2 is given in Table 2. The removal efficiency has been remarkably increased by using such catalyst. With the various pre-treatment of Pt, the valence state of Pt can be changed which ultimately influenced the HCHO removal efficiency (An et al. 2013). MnO_2 have better catalytic efficiency rather than other transition metal oxide. Yu et al. (2011) has made catalyst Pt/MnO_2 to test their performance. They reported that catalytic activity of Pt loading on urchin (support) like MnO_2 vary in a fashion of 2 wt% Pt/urchin like MnO_2 > 1 wt% Pt/urchin-like MnO_2 >> urchin-like MnO_2. Preparation through colloidal deposition route Pt supported iron oxide (Pt/Fe_2O_3) showed excellent catalytic activity and long duration stability over HCHO oxidation (An et al. 2011). An et al. (2013) has prepared Pt/Fe_2O_3 catalyst with several methods like co-precipitation, impregnation, and colloidal-deposition method. They found out that relatively higher catalytic activity for the colloidal deposition method (Pt/Fe_2O_3-CD) among different methods used. Due to its high dispersion degree, Pt could weaken the Fe–O bond presented at the Pt/FeO_x interstitial and ultimately fasten the active oxygen HCHO oxidation. Extremely low Pt content was proved to be the dominant for catalytic oxidation of HCHO at ambient temperature, although practical aspect of this type of catalyst diminishes with the period of time i.e. not active.

Alkali metal ions (like Li^+, K^+ and Na^+) have strong stabilization ability. Pt–O $(OH)_x$-alkali-metal species have stabilized atomic dispersion on the surface of the catalyst and it became an efficient low surface catalyst. Zhang et al. (2012) have shown a low-temperature catalyst z% Na–1% Pt/TiO_2 with varying loadings of Na (z = 0, 1, 2) at a gas hourly space velocity (GHSV) of 12,000 h^{-1}. They found out that HCHO completely conversed at 15 °C while in the case of 1% Na and 0% Na addition the conversion was 96 and 19% at the same temperature respectively. Without Pt, Na can be washed out from TiO_2 surface hence Pt only can have stabilized it on TiO_2. These results can also be reported for Pt/SiO_2 with the addition of alkali ions (Zhai et al. 2010). Due to formation of Pt-$(ONa)_x$ species, Pt species doped by Na were oxidized more as compared to Pt/TiO_2 (Li et al. 2011; Peng and Wang 2007). The result proposed by Zhang, He, and Tanaka (2005) shows that the particle size of Pt is affected by the addition of Na as 10 (Na free), 4.8 (2% Na) and 6.8 Å (1% Na). Addition of alkali metal ion can suppress the Pt–Pt bond in presence of O_2 and deepens atomically dispersed Pt–O species on TiO_2 surface. Most of the work has been proposed on the support of TiO_2 (An et al. 2013; Huang and Leung 2011a, 2011b; Li et al. 2011; Nie et al. 2013; Yu et al. 2011; Zhai et al. 2010; Zhang et al. 2012; Zhu et al. 2011). Different positive influence of alkali metal on Pt/MnO_2 has been analyzed by Chen et al. (2014). To increase the catalytic activity of birnessite and cryptomelane by noble metal support, various studies have been done till now (Liu et al. 2012a; Yu et al. 2011). Chen et al. (2014) has investigated the effect of salts (Na_2CO_3, Na_2SO_4, and $NaNO_3$) over Pt/MnO_2 and found the increasing effect of anions in salt as the following manner: CO_3^{-2} > SO_4^{-2} > NO_3^-. HCHO conversion at 50 °C over the Na_2CO_3 supported catalyst was found 100%. Since, residual anions (SO_4^{-2}, and NO_3^-) were col lected on the surface of Pt/MnO_2 hence effective surface area gets reduced with Na_2SO_4 and $NaNO_3$ which ultimately influence the physiochemical aspects of the catalysts (Wang et al. 2012).

The advantages with using Na_2CO_3 support is that CO_3^{-2} got burn at the higher temperature which ultimately exposed the higher specific surface area and pore volume for increasing catalytic degradation of HCHO oxidation. During practical uses generally all the catalysts adding noble metal which are structurally granular or powder possess great value of pressure drop. They also possess some engineering limitation like dust pollution, removal of nano catalysts with corresponding gases and so on. Hence, due to low pressure drops and forming quality, macroscopically fabricated catalysts are more considerable (Groppi and Tronconi 2005; Kołodziej and Łojewska 2005). Yu et al. (2013) has investigated the diminishment of HCHO over $Au_{0.5}Pt_{0.5}$/MnO_2/cotton catalyst and found that 15 wt% $Au_{0.5}Pt_{0.5}$/MnO_2/cotton possess best performance among 25 wt% $Au_{0.5}Pt_{0.5}$/MnO_2/cotton, 10 wt% $Au_{0.5}Pt_{0.5}$/MnO_2/cotton, and 6 wt% $Au_{0.5}Pt_{0.5}$/MnO_2/cotton. They also reported that cotton surface has gully shape which increases the superficial area of cotton and it does not affect the decomposition of HCHO itself. Cotton fiber just promotes the adsorption of HCHO. Zhang and He (2007) has proposed a comparative data for the catalytic over TiO_2-with 1 wt% noble metal supports (Pt, Rh, Pd, and Au). They resulted in the catalytic activity of Pt/TiO_2 >> Rh/TiO_2 > Pd/TiO_2 > Au/TiO_2 >> TiO_2. They also found that 1 wt% of Pt/TiO_2 catalyst could decompose the HCHO into CO_2 and H_2O in a GHSVs of 50,000 h^{-1} even at ambient temperature. So, format species are potent surface variant on the Pt/TiO_2 and Rh/TiO_2 including with absorbed CO variant in Pt/TiO_2. As in case of Pd/TiO_2 and Au/TiO_2, formation of format species and its degradation into CO is not influencing in nature.

3.1.2 Pd supported noble catalysts

Better thermal stability and comparatively low cost of Pd over precious metal catalysts (like Pt and Au dependent

Table 2: Degradation of formaldehyde with different catalysts at room temperature.

S. no.	Catalysts	Parent material	Inlet condition	Type of reactor	Doping element	Preparation method	Weight (%)	Temperature (ºC)						Time (h)						Result
								20	40	60	80	100	120	1	2	4	6	8	10	
1.	Noble metal catalyst (Zhang and He 2007)	TiO_2	HCHO 100 ppm, He balance, O_2-20 vol%, discharge 50 cm^3/min, GHSVs-50,000/h	Fixed-bed quartz flow reactor	Pt	Impregnation method	1	100	100	100	100	100	100	–	–	–	–	–	–	At ambient condition 100% HCHO conversion obtained with Pt/TiO_2
					Rh		1	20	27	68	100	100	100	–	–	–	–	–	–	
					Pd		1	0	5	22	62	89	100	–	–	–	–	–	–	
					Au		1	0	5	13	37	66	89	–	–	–	–	–	–	
					-		-	0	0	0	0	0	0	–	–	–	–	–	–	
2.	Metal catalyst (Peng and Wang 2007)	TiO_2	HCHO 100 mg/m^3, N_2 balance, O_2 22 vol %, discharge 1200 cm^3/min, GHSV = 300,000 cm^3/gh	Tubular fixed bed flow reactor	Pt	impregnation	0.6 wt%	41	78	94	97	99.25	100	–	–	–	–	–	–	Among all Pt/TiO_2 converts HCHO most effectively with 41% at 20 °C.
					Pd			8.5	14.95	44.47	55	67.23	80.77	–	–	–	–	–	–	
					Rh			8.4	14.5	28.48	48.75	64.40	76.16	–	–	–	–	–	–	
					Mn			3.9	4.67	6.85	10.45	13.69	15.87	–	–	–	–	–	–	
					Cu			0.355	1.12	3.31	6.91	9.08	9.49	–	–	–	–	–	–	
3.	Noble metal catalyst (Peng and Wang 2007)	SiO_2	HCHO 100 mg/m^3, %, N_2 balance, O_2 22 vol%, discharge 1200 cm^3/min, GHSV = 300,000 cm^3/gh	Tubular fixed bed flow reactor	Pt	impregnation	0.6 wt%	9.71	18.28	57.83	76.49	88.81	94.77	–	–	–	–	–	–	SiO_2 found second effective support for Pt in case of degradation of HCHO at room temperature
		$Ce_{0.8}Zr_{0.2}O_2$			Pt	impregnation	0.6 wt%	8.58	9.71	16.42	26.86	37.32	47.38	–	–	–	–	–	–	
		$Ce_{0.2}Zr_{0.8}O_2$			Pt	impregnation	0.6 wt%	5.22	6.72	11.57	14.18	21.27	32.09	–	–	–	–	–	–	
4.	Noblemetal catalyst (Zhang et al. 2014)	TiO_2	HCHO 140 ppm, 25% RH, 20% O_2, GHSV 95,000 h^{-1}, He balance	Fixed-bed quartz flow reactor	2Na–Pd	impregnation	-	–	98.96	99.48	100	100	100	96.77	97.98	97.58	97.58	95.96	97.98	With 2Na–Pd/TiO_2 approximately 100% HCHO decomposition is possible at prescribed inlet condition
					Pd		-	–	72.16	84.53	89.17	92.78	100	–	–	–	–	–	–	
					2Na		-	–	0	0	0	0	0	–	–	–	–	–	–	
					-		-	–	0	0	0	0	0	–	–	–		–	–	
5.	Noble metal oxide (Tang et al. 2006b)	-	HCHO 580 ppm, He balance, O_2 = 18.0%, GHSV = 30,000 mL/(gcat h)	Fixed-bed reactor	Ag/MnO_x–CeO_2	Deposition precipitation	Silver loading of 3 wt%	–	11.81	33.56	68.89	100	100	–	–	–	–	–	–	Conversion into CO_2 from HCHO starts at 40 °C with Ag/MnO_x–CeO_2 catalyst at given inlet condition
					Ag/CeO_2			–	–	–	27.52	75.24	100	–	–	–	–	–	–	
					Ag/MnO_x			–	–	–	19.97	38.69	74.93	–	–	–	–	–	–	
6.	Noble metal catalyst (Li et al. 2016a)	TiO_2	HCHO 140 ppm, 25 °C, 20% O_2, 30% RH, GHSV 190,000 h^{-1}, He balance		$K–Pd/TiO_2$	Impregnation	1 wt% Pd/TiO_2	–	100	100	100	100	100	–	–	–	–	–	–	100% decomposition is achieved with K-Pd/TiO_2 and K-Pd/TiO_2 at 25 °C in given inlet condition
					$Cs–Pd/TiO_2$			–	100	100	100	100	100	–	–	–	–	–	–	
					$Na–Pd/TiO_2$			–	98.45	100	100	100	100	–	–	–	–	–	–	
					$Li–Pd/TiO_2$			–	39.54	61.63	92.25	100	100	–	–	–	–	–	–	
					Pd/TiO_2			–	33.33	44.19	63.57	89.93	98.06	–	–	–	–	–	–	
7.	Noble metal catalyst (Zhang, He, and Tanaka 2005)	TiO_2	HCHO 100 ppm, He balance, O_2 20 vol%, discharge 50 cm^3/min, GHSV 50,000 h^{-1}	Fixed-bed quartz flow reactor (length = 300 mm, diameter = 4 mm)	Pt	Impregnation	1 wt%	–	–	–	–	–	–	100	100	100	100	100	100	100% R.T. conversion of HCHO is obtained with GHSV = 50,000 h^{-1}
			HCHO 100 ppm, He balance, O_2 20 vol%, discharge 50 cm^3/min, GHSV 100,000 h^{-1}					–	–	–	–	–	–	99.57	99.58	99.58	98.29	99.57	97.44	
			HCHO 100 ppm, He balance, O_2 20 vol%, discharge 50 cm^3/min, GHSV 100,000 h^{-1}					–	–	–	–	–	–	97.02	81.71	61.27	60.43	59.14	58.73	
8.	Noble metal catalyst (Li, Zhang, and He 2017)	TiO_2	HCHO 140 ppm, He balance, O_2 20 vol%, 25% RH, GHSV 95,000 h^{-1}	Fixed-bed quartz flow reactor (inlet diameter = 6 mm)	Pd	Impregnation	8 wt% Na	–	82.91	94.31	99.19	100	100	–	–	–	–	–	–	Approximately 100% conversion is gained over 2 wt% Na- Pd/TiO_2 for HCHO at R.T. with GHSV of 95,000 h^{-1}
							4 wt% Na	–	85.69	95.54	99.51	100	100	–	–	–	–	–	–	
							2 wt% Na	–	99.01	99.56	99.82	100	100	96.57	96.95	96.94	97.33	97.71	96.95	
							1 wt% Na	–	88.79	95.85	99.72	100	100	–	–	–	–	–	–	
							1 wt% Pd	–	33.99	57.46	82.16	96.34	100	–	–	–	–	–	–	
							2 wt% Na	–	–	–	–	–	–	98.47	98.47	98.85	98.85	99.62	99.24	

Table 2: (continued)

S. no.	Catalysts	Parent material	Inlet condition	Type of reactor	Doping element	Preparation method	Weight (%)	Temperature (ºC)						Time (h)						Result
								20	40	60	80	100	120	1	2	4	6	8	10	
			HCHO 140 ppm, He balance, O_2 20 vol%, 25% RH, GHSV 80,000 h^{-1}																	
			HCHO 140 ppm, He balance, O_2 20 vol%, 25% RH, GHSV 190,000 h^{-1}				2 wt% Na	–	–	–	–	–	–	73.28	70.99	63.36	60.31	58.02	59.92	
			HCHO 140 ppm, He balance, O_2 20 vol%, 25% RH, GHSV 190,000 h^{-1}				2 wt% Na	–	–	–	–	–	–	89.31	87.02	86.26	86.64	85.5	84.73	
9.	Noble metal catalyst (Tan et al. 2015)	CeO_2(nano-rods)	HCHO 600 ppm, N_2 balance, 20% O_2, GHSV 10,000 h^{-1}	Fixed-bed quartz tubular reactor (4 mm internal 115 diameter)	Pd	Hydrothermal method	0.3 g of nano-rods, 0.005 g of $PdCl_2$	–	5.16	42.62	91.41	–	–	–	–	–	–	–	–	With Pd/ CeO_2(nano-cubes) 100% HCHO is transformed into CO_2 at R.T. with described inlet condition
		CeO_2(nano-octahedrons)					0.3 g of nano-octahedrons, 0.005 g of $PdCl_2$	35.4	74.57	99.56	–	–	–	–	–	–	–	–	–	
		CeO_2(nano-cubes)					0.3 g of nano-cubes, 0.005 g of $PdCl_2$	100	–	–	–	–	–	98.36	100	98.91	95.63	97.27	93.99	
10.	Noble metal catalyst (Zhang et al. 2012)	TiO_2	600 ppm of HCHO, RH 50%, O_2 20 vol%, He balance, discharge 50 cm^3/min, and GHSV 120,000 h^{-1}	Fixed-bed quartz flow reactor	Pt	Impregnation	2% Na, 1 wt% Pt	100	100	100	100	100	100	81.25	83.75	85	86.25	86.25	85	100% alternation is gotten by 2%Na, 1 wt% Pt-TiO_2 even at 20 °C
							1% Na, 1 wt% Pt	96.39	98.45	100	100	100	100	–	–	–	–	–	–	
							1 wt% Pt	19.59	21.13	23.2	27.84	36.08	53.09	–	–	–	–	–	–	
11.	Noble metal catalysts (Chen et al. 2013)	CeO_2	HCHO 80 ppm, 21 vol % O_2/N_2, temperature: 25 °C, RH 50%, GHSV = 34,000 h^{-1}	Continuous flow fixed bed quartz micro-reactor	Au	Deposition–precipitation method	With urea, Au = 1 wt%	–	100	100	100	100	–	34.55	96.34	100	100	–	–	Approx. 100% HCHO could be transformed into Co_2 at R.T with GHSV = 34,000 h^{-1}. over urea, 1 wt% Au/ CeO_2
							DP with NaOH, Au = 1 wt%	–	46.59	95.45	100	100	–	–	–	–	–	–	–	
			HCHO 80 ppm, 21 vol % O_2/N_2, temperature: 25 °C, RH 50%, GHSV = 95,500 h^{-1}				With urea, Au = 1 wt%	–	–	–	–	–	–	94.76	100	100	100	–	–	
			HCHO 80 ppm, 21 vol % O_2/N_2, temperature: 25 °C, RH 50%, GHSV = 143,000 h^{-1}				DP with urea, gold loading of 1 wt%	–	–	–	–	–	–	96.86	100	100	100	–	–	
12.	Noble metal catalysts (An et al. 2013)	MnO_2	HCHO 460 ppm, 21% O_2 and 79% N_2, discharge 50 mL/min, GHSV 20,000 mL/(gcat h), room temperature 298 K	Fixed-bed reactor	$Au_{0.5}$–$Pt_{0.5}$/ cotton support	Co-reduction	6 wt%	0	0	0	1.61	8.47	38.7	–	–	–	–	–	–	15 wt% $Au_{0.5}$–$Pt_{0.5}$/ cotton Support effectively starts the transformation at R.T. and gained 100% degradation at 120 °C.
							10 wt%	0	6.86	22.18	58.87	77.42	85.48	–	–	–	–	–	–	
							15 wt%	0	31.05	57.66	81.05	98.36	100	–	–	–	–	–	–	
							20 wt%	0	15.73	53.63	72.18	87.5	98.73	–	–	–	–	–	–	
							25 wt%	0	25	54.84	75	85.08	90.73	–	–	–	–	–	–	
13.	Metal oxide (Yu et al. 2013)	Fe-oxide	Formalin (an aqueous solution of 37% formaldehyde), flow rate: 6.25 mg of formaldehyde per m^3, space	U-shape glass reactor	Au	Co-precipitation approach	7.10Au/Fe-O	19.41	52.38	82.42	100	–	–	–	–	–	–	–	–	Reaction sufficiently proceed at 20 °C with 100% modification of HCHO at
							4.85Au/Fe-O	15.02	35.16	58.24	82.05	100	–	–	–	–	–	–	–	
							2.52Au/Fe-O	10.62	15.38	27.47	34.79	44.32	100	–	–	–	–	–	–	
							0.73Au/Fe-O	–	–	–	–	–	5.495	–	–	–	–	–	–	
							Reference	–	–	–	–	–	–	–	–	–	–	–	–	

Table 2: (continued)

S. no.	Catalysts	Parent material	Inlet condition	Type of reactor	Doping element	Preparation method	Weight (%)	Temperature (ºC)						Time (h)						Result
								20	40	60	80	100	120	1	2	4	6	8	10	
			velocity of the catalytic combustion is 54,000 h^{-1} mL/g																	100 °C over 7.10 wt % Au/Fe–O catalyst
14.	Transition metal oxide (Shi et al. 2012a)	Ag	HCHO 80 ppm, RH 50%, 21% O_2/N_2 and GHSV = 30,000 h^{-1}	Fixed-bed quartz reactor	-	Co-precipitation method	Ag-MnO_x-CeO_2 mixed oxide (Ag/Mn/Ce = 1:5:4, molar ratio)	–	34.35	44.78	100	100	100	–	–	–	–	–	–	Partial conversion starts at R.T. and 100% transformation occurs at 80 °C Ag–MnO_x–CeO_2 catalyst with
						Incipient wetness impregnation method	Ag/HZ (Si/Al = 500)	–	–	–	48.69	84.78	86.96	–	–	–	–	–	–	Co-precipitation method
15.	Noble metal catalysts (An et al. 2013)	Fe_2O_3	HCHO 100–500 ppm, 20 vol% O_2 N_2 balance	Quartz tube	Pt	Colloid deposition method(CD)	1.0 wt%	100	100	–	–	–	–	–	–	–	–	–	–	CD processed Pt/Fe_2O_3 catalyst converts 100% HCHO at even 20 °C
						Co-precipitation method(Cp)		–	76.21	100	–	–	–	–	–	–	–	–	–	
						Impregnation method(IMP)		–	39.21	80.18	94.27	100	–	–	–	–	–	–	–	
16.	Transition metal oxide (Bai, Arandiyan, and Li 2013)	3D Co_3O_4	HCHO 400 ppm, GSHV = 30,000 mL/(g h), 20 vol% O_2, N_2 balance gas	Fixed bed quartz tube reactor (dia. 10 mm)	–	Hard template method	–	–	–	2.41	4.81	30.93	91.41	99.71	99.43	99.14	99.14	99.14	99.43	Partial conversion of HCHO starts at R.T.
		2D Co_3O_4			–	Hard template method	–	–	–	1.38	1.38	8.59	43.64	70.40	70.69	71.55	72.13	72.41	73.56	approx. 100% conversion over 3D
		Nano Co_3O_4			–	Precipitation method	–	–	–	0.68	1.03	1.37	1.72	0	0	0	0	0	0	Co_3O_4 catalyst prepared by hard template method at 120 °C with GHSV = 30,000 mL/(g h)
		3D Co_3O_4	HCHO 400 ppm, GSHV = 45,000 mL/(g h), 20 vol% O_2, N_2 balance gas		–	Hard template method	–	–	–	2.22	4.43	12.03	59.49	–	–	–	–	–	–	
		3D Co_3O_4	HCHO 400 ppm, GSHV = 60,000 mL/(g h), 20 vol% O_2, N_2 balance gas		–	Hard template method	–	–	–	1.58	2.53	7.28	21.202	–	–	–	–	–	–	
17.	Transition metal oxide (Lu et al. 2016)	MnO_2	HCHO 100 ppm, GHSV = 30,000 mL/(gcat h)	Fixed-bed reactor (length = 500 mm, diameter = 4 mm)	Graphene(G-Mn- 1)	Hydrothermal method	$KMnO_4$ concentration of 1 mg-mL^{-1},	–	31.06	64.59	99.38	100	–	–	–	–	–	–	–	G-MnO_2 hybrid catalyst gained 100% conversion efficiency at 65 °C with concentration of 2 mg/mL
					G-Mn-2		$KMnO_4$ concentration of 2 mg/mL	–	34.78	87.58	100	100	–	98.86	–	–	–	–	–	
					G-Mn-3		$KMnO_4$ Concentration of 3 mg/mL	–	24.83	32.29	77.02	100	–	–	–	–	–	–	–	
					MnO_2			–	24.84	59.63	71.43	82.61	–	–	–	–	–	–	–	
					G			–	0	0	0	0	–	–	–	–	–	–	–	
18.	Transition metal oxide (Chen et al. 2007)	MnO_X	100 ppm HCHO, 20 vol % O_2, He balance gas, discharge 50 cm^3/min GHSV = 50,000 h^{-1}	Fixed-bed Quartz flow Reactor (length) 300 mm, (diameter) 4 mm	K_XMnO_2 Honeyco Mb Nanosphere		70 mg	4.8	9.6	61.6	100	100	–	–	–	–	–	–	–	HCHO is partially converted at R.T. and approx. 100% degradation could be gained at 80 °C over K_XMnO_2
					K_XMnO_2 Hollow Nanospheres		50 mg	4.8	6.4	23.2	79.2	100	–	–	–	–	–	–	–	

Table 2: (continued)

S. no.	Catalysts	Parent material	Inlet condition	Type of reactor	Doping element	Preparation method	Weight (%)	Temperature (ºC)						Time (h)						Result
								20	40	60	80	100	120	1	2	4	6	8	10	
					Reference		–	0	0	0	0	0	–	–	–	–	–	–	–	Honeycomb Nanosphere catalyst
19.	Transition metal oxide (Xingfu et al. 2006)	MnO_X	O_2 20.0%, He balance gas, discharge 80 mL/min	Quartz tube Reactor (diameter = 6 mm)	Octahedral molecular sieve(OMS-2) nanorods		Molar composition of $MnSO_4 \cdot H_2O$, $KMnO_4$, and $K_2S_2O_8$ was 39:28:1	–	–	9.87	100	–	–	–	–	–	–	–	–	At 70 °C complete oxidation of HCHO takes place over octahedral molecular sieve (OMS-2) nanorods
					MnO_X		-	–	–	24.07	100	100	–	–	–	–	–	–	–	–	
20.	Transition metal oxide (Chen et al. 2014)	Pt/ MnO_2	HCHO 200 ppm of HCHO, discharge 50 mL/min GHSV = 30,000 mL/(gcat h)	Quartz tubular fixed-bed reactor	Na_2CO_3	Impregnation process	2 wt% Na, 1 wt% Pt	–	72.34	100	100	100	–	–	–	–	–	–	–	Fractional oxidation of HCHO acquired at R.T. and 100% complete oxidation occurred at apprx. 50 °C over Na_2CO_3 synthesized Pt/MnO_2 catalyst
					Na_2SO_4			–	49.16	81.68	90.65	100	–	–	–	–	–	–	–	–	
					$NaNO_3$			–	37.19	71.96	80.56	100	–	–	–	–	–	–	–	–	
					Without alkali metal			–	39.81	71.96	89.91	100	–	–	–	–	–	–	–	–	
21.	Noble metal catalyst (An et al. 2013)	MnO_2	HCHO 460 ppm, discharge 50 mL/min, GHSV = 20,000 mL/(gcat h), urchin-like MnO_2	Fixed-bed reactor	Pt	Reflux method	0 wt%	10	34.71	65.88	89.41	96.47	100	–	–	–	–	–	–	Partial catalytic oxidation started at R.T. and total elimination of HCHO occurred at 70 °C over 2 wt% Pt catalyst supported with nest like MnO_2
							0.5 wt%	30	62.94	84.12	91.76	99.4	100	–	–	–	–	–	–	
							1 wt%	30	61.18	96.47	99.41	100	100	–	–	–	–	–	–	
							2 wt%	16.47	39.41	68.82	97.65	100	100	–	–	–	–	–	–	
							3 wt%	0	0	2.94	14.71	32.94	46.47	–	–	–	–	–	–	
			Cocoon-like MnO_2			Redox reaction	-	0	0	3.57	3.57	17.86	37.24	–	–	–	–	–	–	
			Urchin-like MnO_2			Reflux method		0	0	2.55	14.29	32.14	46.94	–	–	–	–	–	–	
			Nest-like MnO_2			Hydrothermal method		0	0	2.55	14.29	41.33	61.73	–	–	–	–	–	–	
			Cocoon-like MnO_2		Pt		2 wt%	24.54	69.48	83.62	95.88	100	–	–	–	–	–	–	–	
			Nestlike MnO_2		Pt		2 wt%	41.44	79.79	97.53	100	100	–	–	–	–	–	–	–	
22.	Transition metal oxide (Xu et al. 2014a, 2014b)	CeO_2	HCHO 810 ppm, 50 mg catalyst, 20% O_2, N_2 balance gas, GHSV = 84,000 h^{-1}	Fixed-bed quartz tube reactor of 9 mm internal diameter containing 50 mg of catalyst powder mixed with quartz sand	Ag/CeO_2-N	Hydrothermal method	2 wt%	–	–	13.73	29.08	68.3	100	–	–	–	–	–	–	Hydrothermally fabricated Ag/CeO_2-N catalyst converted partial HCHO at R.T. and 100% abatement of HCHO occurred at 120 °C
					CeO_2-N		2 wt%	–	–	2.61	3.59	5.88	9.47	–	–	–	–	–	–	
					Ag/CeO_2-P	Wet impregnation method	2 wt%	–	–	3.27	3.92	8.49	19.28	–	–	–	–	–	–	
					CeO_2-P		2 wt%	–	–	2.61	3.59	5.88	9.48	–	–	–	–	–	–	
23.	Transition metal oxide (Zhang et al. 2015b)	TiO_2 Al_2O_3 CeO_2	HCHO 110 ppm, 20% O_2, N_2 Balance gas, GHSV = 100,000 mL/(gcat h)	Fixed-bed quartz flow reactor (inlet dia = 4 mm)	Ag	Solution impregnation	8 wt%	–	9.54	40.24	86.16	97.88	98.94	–	–	–	–	–	–	Ag/TiO_2 showed better oxidative activity at R.T. with apprx. 100% conversion of HCHO at 95 °C
							8 wt%	–	7.77	19.43	63.6	87.63	99.29	–	–	–	–	–	–	
							8 wt%	–	7.06	16.96	39.22	61.48	71.02	–	–	–	–	–	–	
24.	Mixed oxide catalyst (Shi et al. 2012b)	Co–Mn oxides			CoMn(3/1)	Coprecipitation method	Atomic ratio of Co/Mn = 3/1	–	13.22	44.83	–	–	–	61.22	100	100	100	100	100	Co–Mn oxide catalyst could do partial oxidation of HCHO at R.T. and can exactly oxidize at apprx. 75 °C
					CoMn(3/1)	Citric acid method	Atomic ratio of Co/Mn = 3/1	–	3.45	15.52	28.74	99.43	–	–	–	–	–	–	–	
					MnO_X			–	4.59	15.52	69.52	–	–	–	–	–	–	–	–	
					Co_3O_4			–	0.57	7.47	24.71	89.66	–	–	–	–	–	–	–	
25.	Transition metal oxide catalyst	OMS-2	HCHO 500 ppm, 10 vol % O_2, N_2 balance gas, flow rate 100 cm^3/	Fixed-bed quartz flow reactor (8 mm in diameter)	Pt/OS-2	Impregnation method	1 wt%	–	0	16.37	33.45	50.18	100	–	–	–	–	–	–	Addition of Pt over OMS-2 support could oxidize HCHO at low temperature
					Pt Ce/OMS-2		1 wt%	–	–	0	16.73	36.65	51.25	–	–	–	–	–	–	
					OMS-2		-	–	–	–	0	39.86	100	–	–	–	–	–	–	
					Ce/OMS-2		1 wt%	–	–	–	–	0	23.84	–	–	–	–	–	–	

Table 2: (continued)

S. no.	Catalysts	Parent material	Inlet condition	Type of reactor	Doping element	Preparation method	Weight (%)	Temperature (ºC)						Time (h)						Result
								20	40	60	80	100	120	1	2	4	6	8	10	
	(Wang and Li 2009)		min, GHSV 30,000 cm^3/g h			Refluxing method														and it could gained 100% oxidation efficiency at 120 °C
26.	Transition metal oxide catalyst (Bai and Li 2014)	Co_3O_4	Discharge 100 mL/min, HCHO 100 ppm, 20% (vol) of O_2, N_2 balance gas, GHSV = 30,000 h^{-1}	Fixed bed quartz tube reactor (diameter = 10 mm)	K-Ag/Co_3O_4	Impregnation method	K (1.7 wt %),Ag (8.2 wt %)	–	62.23	81.14	100	100	–	–	–	–	–	–	–	55% removal efficiency has achieved with K-Ag/Co_3O_4 at
					K-Ag/Co_3O_4		K (0.9 wt%), Ag (8.2 wt%)	–	23.22	51.06	100	100	–	–	–	–	–	–	–	room temperature with given condition
					Ag/Co_3O_4		Ag (8.2 wt%)	–	3.92	29.06	71.27	100	–	–	–	–	–	–	–	and complete elimination at 80 °C
					3D-Co_3O_4		Ag (8.2 wt%)	0.33	1.67	33.55	90.12	–	–	–	–	–	–	–	–	
27.	Transition metal oxide catalyst (Li et al. 2016b)	MnOx	HCHO 400 ppm gaseous, O_2 21%, N_2 balance gas, discharge 100 mL/min	Fixed-bed reactor	Ag/Fe0.1–MnO*x*	One-pot synthesis method	Fe/Mn = 0.1, molar ratio	–	54.3	78.13	98.05	100	–	–	–	–	–	–	–	100% conversion efficiency is gained
					Ag/Fe0.05–MnO*x*		Fe/ Mn = 0.05, molar ratio	–	49.22	69.53	91.8	100	100	–	–	–	–	–	–	with Ag/Fe0.1–MnO*x* at specified condition
					Ag/MnO*x*		–	–	37.89	51.17	74.61	88.28	100	–	–	–	–	–	–	
					Fe0.1–MnO*x*		Fe/Mn = 0.1, molar ratio	–	9.38	12.5	22.27	31.25	54.29	–	–	–	–	–	–	
28.	Noble metal catalyst (Park et al. 2012)	Zeolite	HCHO 40 ppm gaseous, 20% O_2, 3% H_2O, Ar balance gas	Packed-bed flow reactor	Pd	Incipient wetness impregnation	0.1 wt%	–	25.37	44.12	60.29	80.15	88.34	–	–	–	–	–	–	Approximate 100% elimination is achieved with 0.5 wt% loading at 40 °C
							0.25 wt%	–	80.15	91.18	96.69	100	100	–	–	–	–	–	–	
							0.5 wt%	–	95.22	100	100	100	100	–	–	–	–	–	–	
29.	Noble metal catalyst (Liu et al. 2012c)	CeO_2–Co_3O_4	8 ppm of HCHO, GHSV 1.5 × 104 mL/h g	Continuous flow fixed-bed reactor	Au	Gas bubbling assisted DP	1 wt%	–	18.82	41.94	82.79	100	–	–	–	–	–	–	–	Apprx. Complete elimination is achieved with 3 wt%
							2 wt%	–	49.46	76.88	–	–	–	–		–	–	–	–	
							3 wt%	–	100	–	–		–	–	–	–	–	–	–	
							4 wt%	–	89.24	100	–	–	–	–	––		–	–	–	
30.	Noble metal catalyst (Huang and Leung 2011b)	TiO_2	HCHO 10 ppm, RH 50%, GHSV = 80,000 h^{-1}	Fixed-bed reactor	Pt	Impregnation	0.1 wt% PtO	–	–	–	–	–	–	25.31	5.39	5.39	5.39	5.39	5.39	Complete elimination at room temperature is gained with 0.1 wt% Pt
							0.1 wt% Pt	–	–	–	–	–	–	98.76	100	100	100	100	100	
							1 wt% PtO	–	–	–	–	–	–	61	29.88	25.73	25.73	25.73	25.73	
							1 wt% Pt	–	–	–	–	–	–	98.76	100	100	100	100	100	

catalysts) make it beneficial of use. But it requires a high temperature for oxidation. 1% of Pd nanoparticles can efficiently oxidize HCHO at ambient temperature (Vijayakrishnan et al. 1992). Huang et al. (2013a) have also found out that the deposition precipitation method is more capricious than the impregnation method in the case of Pd/TiO_2 catalysts due to larger capacity for production and transfer of chemisorbed oxygen. The removal efficiency of HCHO with Pd wt% in the case of impregnation method shows the trend in the following manner: 8.5, 93.2, and 19% removal efficiency for 0.1, 0.5, and 1% Pd. Expensive cost of Pd limits the high Pd loading. Alkali metal as an electronic or textural conductor prefers as a catalyst for several catalytic processes including NO (Xu et al. 2014a, 2014b) and CO oxidation (Mirkelamoglu and Karakas 2006; Yentekakis et al. 1994). Zhang et al. (2014) has conducted a test on 2Na–Pd/TiO_2 catalyst at a GHSV of 95,000 h^{-1}. They found out that 100% HCHO decomposition into CO_2 and H_2O at 25 °C with a feed concentration of 140 ppm of HCHO. Result proves that Na species act as an inductor and stabilizer for negatively charged and well-dispersed Pd variants that promotes water and chemisorbed oxygen's activation.

A series of alkali metal (K, Li, Na and Cs) doping have investigated on Pd/TiO_2 support by Li et al. (2016b). They resulted in K > Cs > Na > Li like the trend in the condition of 550 ppm HCHO and a GHSV of 640,000 h^{-1} over Pd/TiO_2 support. The highest Pd dispersion degree with active sites is showing by K-Pd/TiO_2 catalyst among all in ambient temperature HCHO oxidation. Li, Zhang, and He (2017) have reported the optimized value of loading at Pd/TiO_2 support is 2 wt% in a GHSV range of 80,000–190,000 h^{-1} and RH of 25–65%. They found an activity trend of 2.0 Na–Pd/TiO_2 > 1.0 Na–Pd/TiO_2 > 4.0 Na–Pd/TiO_2 > Pd/TiO_2 among the different loadings of sodium. Galvan et al. (Huang et al. 2013b) has reported that total combustion of HCHO had achieved at 220 °C temperature over 18.2% Mn/Al_2O_3 catalyst. But due to the addition of 0.1% Pd this temperature gets reduced to 90 °C (Álvarez-Galván et al. 2004). At the surface of Pd–Mn/Al_2O_3, several activities have involved for the decomposition of HCHO. The relative rates are PdO > MnO_x >> Al_2O_3. Interstitial oxygen of the PdO cluster has high activity in oxidation of HCHO (Cordi and Falconer 1996).

3.1.3 Supported gold catalysts

Earlier gold was assumed as the poor heterogeneous catalyst due to its electronic structure. However, after the discovery of Haruta et al. (1989), highly dispersed particles of metallic gold permit co-oxidation at relatively low temperatures. This was just the initiation of the application of gold as the catalyst. Gold catalysts have been reported as active catalysts in hydrogenation of carbon oxide, in water gas shift reaction and most importantly in oxidation of VOCs (Delannoy et al. 2010; Dobrosz-Gómez, Kocemba, and Rynkowski 2008; Hosseini et al. 2012; Wang et al. 2011; Yi et al. 2010a, 2010b). In spite of the high-temperature requirement for total oxidation of HCHO, Fe_2O_3-, CeO_2-, and ZrO_2-supported Au has been proved as an active catalyst (Hong et al. 2010; Li et al. 2007). Chen et al. (2013) has prepared Au/TiO_2 catalyst by two methods i.e. deposition precipitation (DP) with urea and with NaOH to examine the catalytic activity of Au/TiO_2 for decomposition of HCHO oxidation. They reported that Au/CeO_2 (DPU prepared) shows higher catalytic activity than Au/CeO_2 (prepared through DPN) due to higher active surface oxygen variant even at high GHSV of 143,000 h^{-1}. It has been illustrated that presence of Au weakens surface Ce–O bond (Scire et al. 2003; Serre et al. 1993). Li et al. (2008) have prepared a series of gold /iron-oxide catalysts for the decomposition of HCHO through co-precipitation method. They critically observed the decomposition of HCHO by varying the Au loading from 0.73, 2.52, 4.85 to 7.10 wt% on gold iron supported catalysts and found that 7.10 wt% of gold content showed highest catalytic activity.

They suggested that gold species exist in fractional charged gold atoms ($Au^{\delta+}$ where $\delta < 1$) which is a transition state between cationic gold (Au^+) and metallic gold. Liu et al. (2012a) have fabricated 3-D ordered macro-porous (3DOM) Au/CeO_2 catalyst with a different process named colloidal crystal template process joined with a precursor complexion technique. They noticed that 3DOM Au/CeO_2 catalysts decomposes 30% HCHO at ambient temperature and 100% decomposition showed at ~75 °C for ~0.56 wt% of Au. Mutually connected spherical voids promoting the less aggregation and fine dispersion of Au nanoparticles may credit for their improved catalytic activity for the 3DOM structure of Au/CeO_2. Deactivation of 3DOM Au/CeO_2 catalyst happened due to formation of carbonate and hydrocarbon at eon surface of 3DOM Au/CeO_2. For enhancement of result, another test using 3DOM Au/CeO_2–Co_3O_4 catalysts fabricated through precursor thermal decomposition assisted colloidal templating technique has carried out (Liu et al. 2012a). The result shows that catalyst 3DOM Au/CeO_2–Co_3O_4 acquired proper 3DOM shape with adjustable pore sizes. Their phase structures, compositions, and elemental valence state on the surface can be monitored by regulating the molar ratio (Ce/Co). With the help of thermal decomposition of Ce and Co oxalate precursor, the nanowalls pore size of 3–4 nm were made in 3DOM Au/CeO_2–Co_3O_4. They achieved 100%

decomposition of HCHO at ~39 °C for 3DOM Au/CeO_2–Co_3O_4 catalyst.

3.1.4 Supported silver catalyst

The different oxidation states of silver (Ag) permit it to use with different supports. Zhang et al. (2015b) has used different supports (TiO_2, Al_2O_3, and CeO_2) for analyzing their catalytic activity doped with Ag. Results show that Ag/TiO_2 exhibit superior catalytic activity among them with 100% oxidation of HCHO at 95 °C followed by 110, 125 °C by Ag/Al_2O_3 Ag/CeO_2 respectively. TiO_2, Al_2O_3, and CeO_2 have approximately equal activation energy but high dispersion degree of silver and size factor over supports create a difference. Tang et al. (2006a) have used the mixed oxide (MnO_x–CeO_2) doped with Ag to improve catalytic activity of mixed oxides. Result shows that due to oxygen transfer mechanism 100% oxidation of HCHO takes place at 373 K over Ag/MnO_x–CeO_2 catalyst. To use the silver more effectively Bai and Li (2014) has prepared 3D-Ag/Co_3O_4 with addition of K^+ ions catalyst. Result shows that addition of Ag into 3D-Co_3O_4 decreases the conversion temperature to 110 °C in GHSV of 30,000 h^{-1}.

3.2 Reaction mechanism and pathway for catalytic oxidation of formaldehyde

A generalized reaction mechanism is not illustrated because of characteristic of HCHO molecule and catalyst is the factors on which the legitimacy of every mechanism depends. For VOC_s oxidation, there are possibly three mechanisms i.e., Eley–Rideal, Langmuir–Hinshelwood and Mars–Van Krevelan (Liotta 2010; Ordóñez et al. 2002).

As per the *L–H* mechanism, kinetics of reactions between the solid and gas phase can be quantitatively treated (Lam et al. 2007). According to this, the surface reaction between initial contaminants and oxidizer (absorbed molecules) is the basic process. In the *E–R* mechanism, the gas phase absorbed particle retaliates with contaminant particles. Further, in case of the MVK mechanism, it is two-stage redox reaction mechanisms that involve the oxidation and reduction of VOC particles and oxygen. The redox states of the MVK mechanism are as follows.

(a) First, catalysts will be oxidized by oxygen in gas phase to create an oxygen adsorption site (O). This (O) reacts with the absorbed particles or contaminants in the air.
(b) Simultaneously in the 2nd step pollutant molecules will reduce the oxidized catalyst (Ding et al. 2006).

The following are the two steps

$$O_2 + () \xrightarrow{k_o} (O_2) \xrightarrow{()} 2(O) \tag{17}$$

$$R + (O) \xrightarrow{k_i} CO_2 + H_2O + () \tag{18}$$

where k_o represents as the oxygen rate constant, k_i represents as constant for surface reaction rate, and blank symbol () depicts an oxygen adsorption site.

Generally, MVK mechanism is broadly applied for HCHO oxidation over platinum catalysts (Liu et al. 2012a). Rapid formation of format species from the oxidation of HCHO is a major step for conversion into CO_2 and H_2O is performed in two steps i.e.

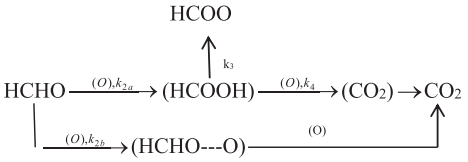

(19)

With

$$O_2 + () \xrightarrow{k_i} (O_2) \xrightarrow{()} 2(O) \tag{20}$$

In case of Pt/TiO_2, at metal-support interface, after the formation of oxygen vacancies, oxygen absorbed on the active sites with packing the vacancy by oxygen molecule and coordinating with the Ti^{4+} as an adatom (Alexeev et al. 2005). The formation of a high intensity of oxygen species greatly influences the oxidation reaction. For sodium-free Pt/TiO_2 catalysts, the reaction mechanism includes the formation of formate species which is purely degraded into CO species (Zhang, He, and Tanaka 2006). This formed CO species ultimately converted into CO_2 after exposure of the catalyst to O_2 and finally CO_2 leaves the surface. So the reaction mechanism includes the following steps for the decomposition of HCHO into CO_2 i.e.

$$HCHO \rightarrow HCOO^- \rightarrow CO \rightarrow CO_2 \tag{21}$$

In the decomposition process, rate demonstrative step is the conversion of formate into CO. Zhang et al. (2012) has studied reaction mechanism of decomposition of HCHO into CO_2 over Sodium doped Pt/TiO_2 catalyst with using in situ DRIFTS. They reported that on the surface of the catalyst, two types of surface (OH) groups were formed at 3695 and 3600 cm^{-1}. After 60 min, a complete reaction occurred between active OH groups and formate because of the disappearance of $HCOO^-$ species from the base.

Results show a new pathway for 2% Na–1% Pt/TiO_2 catalyst i.e.

$$HCHO \rightarrow HCOO \rightarrow OH \rightarrow H_2O + CO_2 \quad (22)$$

This reaction gives a new preferable path for the decomposition of HCHO into CO_2 i.e. surface hydroxyls and formate reaction are preferred rather than degradation of formate into CO. Zhang, He, and Tanaka (2006) have also proposed two different paths for the decomposition process which are when deficiency of OH group occurs on the catalyst surface, the formation of surface CO starts from formate species.

$$HCOO - M \rightarrow OH - M + CO - M \quad (23)$$

But in the case of an abundant amount of OH groups present, decomposition of formate into CO_2 takes place.

$$HCOO - M + OH - M \rightarrow H_2O + CO_2 + 2M \quad (24)$$

A similar result has given by Zhang, He, and Tanaka (2006) that in case of Pt/TiO_2 and Rh/TiO_2 catalysts, effective surface species are formate species along with absorbed CO molecules on Pt/TiO_2.

$$H_2CO_3 \Leftrightarrow CO_2(g) + H_2O \quad (32)$$

Liu et al. (2012a) has further explained the reaction mechanism of 3DOM Au/CeO_2 the catalyst for enhancing the catalytic oxidation of HCHO. They explained the reaction mechanism in two steps catalyzed with ionic Au^{3+} and metallic Au^0 and suggested that higher catalytic performance has shown by ionic Au^{3+}. Hereafter adsorption of HCHO takes place onto the CeO_2 surface. This process includes the formation of HCOOH and Au^0 with the transformation of active oxygen from Au_2O_3. Now formate species would be formed due to the interaction of CeO_2 and HCOOH. CO_2 would be produced with the complete oxidation of HCOOH. Chen et al. (2013) has elucidated the reaction intermediate using in situ DRIFTS for Au/CeO_2 catalysts. They also gave a similar reaction for decomposition of HCHO into CO_2 which involves four basic steps for the decomposition. The first major step includes the formation of formate species due to oxidation of HCHO in the deficiency of O_2 and/or H_2O.

$$HCHO \xrightarrow{Pt,Rh>>Pd>Au,[O]} HCOOH - M \xrightarrow{Pt>Rh>>Pd>Au} HCOO - M \xrightarrow{Pt>Rh} CO - M + H_2O$$
$$\downarrow {}^{,O_2}$$
$$CO_2 + M \quad (25)$$

Figure 5 order of the reaction for catalytic degradation of HCHO on the noble metal (Au, Pd, Rh, and Pt) catalyst supported with TiO_2.

Ma et al. (2011) has further defined the steps of catalytic reaction over $Au/Co_3O_4–CeO_2$ catalyst. The first step has defined for reaction is adsorption of HCHO on surface of Co_3O_4. •CHO species on surface forms due to adsorption of HCHO.

$$Co^{3+} + HCHO \rightarrow Co^{2+} + \bullet CHO + H^+ \quad (26)$$

$$\bullet CHO + O^{*-} \rightarrow HCOO\bullet^- \quad (27)$$

$$HCOO\bullet^- + H^+ \rightarrow HCOOH \quad (28)$$

$$Co^{3+} + HCOOH \rightarrow Co^{2+} + HCOO \bullet + H^+ \quad (29)$$

Now (*C–H*) formate is attacked by active surface oxygen to form bicarbonate (HCO_3^-) species, and this bicarbonate (HCO_3^-) will meet with H^+ to form carbonic acid. CO_2 will form due to dissociation of H_2CO_3 which is shown in Figure 5.

$$HCOO\bullet^- + O^{*-} \rightarrow HCO_3^-\bullet \quad (30)$$

$$HCO_3^{*-} \bullet + H^+ \rightarrow H_2CO_3 \quad (31)$$

$$HCHO(ad) + [O]_S \xrightarrow{k1} H^+ + \left[HCOO^-\right]_S + []_S \quad (33)$$

In water containing feed gas, generation of hydroxyl groups absorbed the HCHO and then these OH groups oxidize the reactant.

$$HCHO(ad) + [OH]_S \xrightarrow{k_1'} \left[HCOO^-\right]_S + H^+ \quad (34)$$

Now hereafter oxidation of equations (33) and (34) could form CO_2 on Au/CeO_2 catalyst.

$$\left[HCOO^-\right]_S + [O]_S + H^+ \xrightarrow{k_2} H_2O + CO_2 + 2[] \quad (35)$$

$$\left[HCOO^-\right]_S + [OH] \xrightarrow{k_2'} CO_2 + H_2O \quad (36)$$

Tang et al. (2006b) has investigated the catalytic oxidation of HCHO over $Ag/MnO_x–CeO_2$ catalysts. For oxidation purposes, he used CeO_2 which is famous for the oxygen equipped catalyst. They proposed the mechanism in a way that oxidation of HCHO is performed with the oxygen released due to the degradation of Ag_2O. Further, the formation of Ag_2O is continuously achieved through the re-oxidation of Ag from MnO_2 and oxygen from CeO_2 regenerate

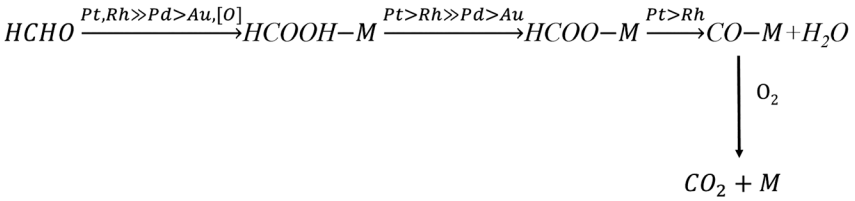

Figure 5: Order of the reaction for catalytic degradation of HCHO on the noble metal (Pt, Rh, Pd and Au) catalyst supported with TiO_2 (Zhang and He 2007).

the Mn_2O_3 to MnO_2. Simultaneously re-oxidation of CeO_2 from Ce_2O_3 is formed through the oxygen of feed gas.

3.3 Metal oxide catalysts used in catalytic oxidation

After searching alternate to noble metal some metal oxide and transition metal oxides found as an active substitute (Reed and Ceder 2004). Due to different valence state and electronic configuration catalysts made through transition metal oxide possess strong catalytic activity for decomposition of volatile organic pollutants (Gluhoi, Bogdanchikova, and Nieuwenhuys 2005; Popova et al. 2010; Sinha et al. 2008; Wang and Li 2010). For VOCs oxidation, metal oxides play a strong role such as manganese, chromium, cobalt, copper, silver, iron, vanadium, and nickel. These are relatively cheaper catalysts with noble catalysts.

3.3.1 MnO_x support

There are generally two forms available of MnO_x i.e. cryptomelane and birnessite. It was investigated that MnO_x shows a strong influence to decompose HCHO at low temperatures. Crptomelane type MnO_2 is chemically made of mixed-valence state of manganese (Mn^{4+}, Mn^{3+} and Mn^{2+}) and physically composed of big open layers or channels (Villegas et al. 2005). Tang et al. (Xingfu et al. 2006) have synthesized manganese oxide octahedral molecule sieve (OMS-2) nanorods for decomposition of HCHO formaldehyde at a lower temperature. They observed that 100% conversion at 353 K temperature with neglecting the intermediates such as CO and formic acid. For MnO_x powder the temperature required for the degradation of MnO_x was found at 373 K which ultimately proves the morphological impact. Chen et al. (2007) has conducted a test for the decomposition of HCHO with monodisperse manganese oxide honeycomb and hollow nanospheres. They have compared the test result with manganese oxide octahedral molecular sieve (OMS-2) nanorod. The decreasing order of catalytic activity over HCHO decomposition as hollow K_xMnO_2 nanospheres > honeycomb K_xMnO_2 nanospheres > OMS-2 nanorods > MnO_x powders. Chen et al. (2009) had evaluated the complete oxidation of HCHO over different tunnel structure of manganese oxides which are: pyrolusite, crptomelane, and todorokite. They had shown that complete conversion of HCHO into CO_2 and H_2O can be achieved through 2 × 2 manganese oxide with the crystal tunnel size of 0.46 × 0.46 nm^2 at 140 °C. However, the conversion is limited to 20 and 40% for 1 × 1 and 3 × 3 manganese oxide with the 0.23 × 0.23 and 0.69 × 0.69 crystal tunnel size. Tian et al. (2012) had evaluated catalytic activity of birnessite type manganese oxides prepared through the microemulsion process. They have taken BSW-100, BSW 120, and BSW-140 (manganese oxide products by heating 60, 100, 120, and 140 °C) catalyst to examine their catalytic properties over HCHO oxidation. They reported that at 100 °C BSW-120 conversion rates are about 100% which showed that BSW-120 is a better catalyst for HCHO decomposition. Manganese oxides reduce in the following steps:

$$MnO_2 \rightarrow Mn_2O_3 \rightarrow Mn_3O_4 \rightarrow MnO \tag{37}$$

Jingjing et al. (Pei, Han, and Lu 2015) has prepared a hopcatile catalyst ($CuO–MnO_2$) to examine the removal efficiency of indoor formaldehyde. They found that at room temperature (25 °C, 50% RH, and 180 ppb concentration level indoor) removal efficiency was 30% which is a quite good removal performance at room temperature. The proposed reaction process over CuO/MnO_2 between oxygen and formaldehyde as follows:

$$HCHO + * \xleftrightarrow{K_{HCHO}} HCHO^* \tag{38}$$

$$O_2 + * \xleftrightarrow{K_{O_2}} O_2^* \tag{39}$$

$$HCHO^* + O_2^* \xrightarrow{K} CO_2^* + H_2O^* \tag{40}$$

$$H_2O^* \xleftrightarrow{K_{H_2O}} H_2O + * \tag{41}$$

$$CO_2^* \xleftrightarrow{K_{CO_2}} CO_2 + * \tag{42}$$

where K = reaction ppbm/s; K_{HCHO}, K_{H_2O}, K_{O_2}, and K_{CO_2} are the absorption equilibrium constant respectively ppb^{-1}.

A hybrid catalyst based on graphene–MnO_2 has been examined as a new catalyst for effective low-temperature oxidation of HCHO by Lu et al. (2016). This hybrid designed catalyst showed strong removal efficiency and indicating a much low 100% removal at 65 °C temperature. They have resulted that the incorporation of graphene nanosheet exposes not only active surface but also promoted a large

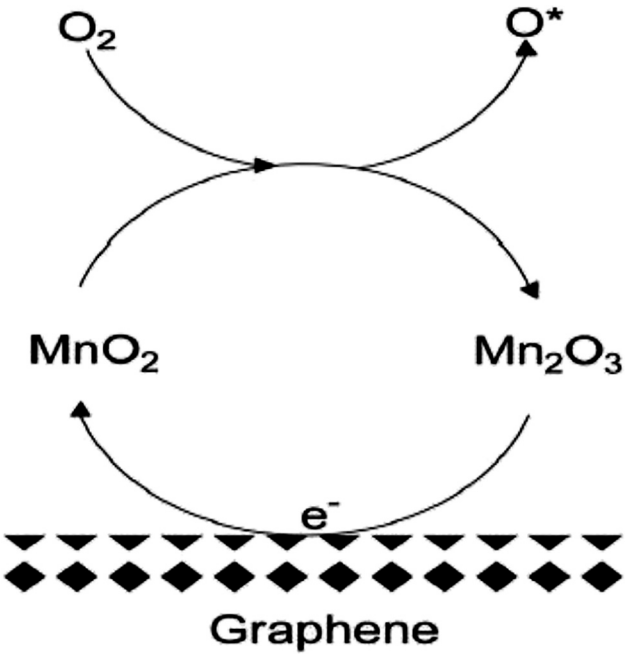

Figure 6: Oxidation of manganese oxide on graphene support (Lu et al. 2016).

amount of OH^{-1} surface species as given in Figure 6 (Lu et al. 2016).

3.3.2 Co oxide catalyst

Co_3O_4 let strong catalytic performance for a different field. Bai, Arandiyan, and Li (2013) has performed a comparative study on nano-Co_3O_4, 3D-Co_3O_4 and 2D-Co_3O_4 for catalytic oxidation of HCHO at 400 ppm HCHO concentration and GHSV of 30,000 mL/(g h). At 130 °C complete conversion of HCHO is getting through 3D-Co_3O_4 in space velocity of 30,000 mL/(g h) and termed as best the catalyst among all. They found that 3D-Co_3O_4 has best catalytic activity among 2D-Co_3O_4 and nano-Co_3O_4. They found that the stability of HCHO conversion is also long when tested over 160 h. Ma et al. (2011) has evaluated the performance of Co_3O_4–CeO_2 and Au/Co_3O_4–CeO_2 which was made through the nano casting method. The evidence of the test result clearly shows the effect of morphology. Mesoporous nanocasted Co_3O_4 catalyst yield CO_2 about 20.3% at 25 °C in contrast to 2.5% CO_2 through Co_3O_4 which were made through the precipitation method.

3.3.3 Al_2O_3 catalyst

Due to high surface area of Al_2O_3, Zhang and He (2005) have used it for catalytic oxidation of formaldehyde at room temperature. The observation shows that no catalytic oxidation of formaldehyde takes place at room temperature in CO_2, but at the catalyst surface adsorption takes place. When adsorption reached to saturation point at the catalyst surface, the intensity of HCHO decreased to zero. The time of conversion of formaldehyde to CO_2 decrease as 2100–700 and 400 min as the increase GHSV 10,000–30,000 and 50,000 h^{-1}.

3.3.4 Mixed oxide catalyst

Li et al. (2014) has worked on the mixed oxide catalyst and investigated the catalytic activity for $Mn_xCe_{1-x}O_2$ (x varies like 0.3, 0.5, 0.7, and 0.9) for the removal of HCHO. They prepared $Mn_xCe_{1-x}O_2$ with different methods (pechini) from trend and observed that for x = 0.5, 100% removal efficiency has found at 270 °C for GHSV of 10,000 h^{-1}. They arranged the result in the varying Mn fraction. The trend follows: T100 (100% completion at temperature) values are 285, 270, 295, and 310 °C for x = 0.3, 0.5, 0.7, and 0.9 for catalyst $Mn_xCe_{1-x}O_2$. The decomposition of formaldehyde due to different catalyst is given in Table 2 at room temperature.

3.4 Operating parameter for catalytic oxidation

For preparing strong influencing catalysts and increasing removal efficiency of HCHO, it is important to understand significance of the operating parameter of catalytic oxidation. Catalytic activity is directly affected through operating parameter hence optimized value is mandatory.

3.4.1 Effect of relative humidity

Atmospheric moisture promotes catalytic activity of HCHO oxidation. This has been verified through the diffuse reflectance infrared Fourier transform (DRIFT) that presence of moisture improves performance of the hydroxyl group. There have been found some contradictory reports that indoor moisture blocks the active site by adsorbing on them at low temperatures (Skrobot et al. 2003). The un stable condition for the catalyst is arisen due to presence of H_2O_2 which helps in thorough loss of activity. In another literature, it has been found that presence of indoor moisture depreciated catalytic activity of TiO_2 supported gold catalyst (Bollinger and Vannice 1996). However, Kwon et al. (2015) have reported that in presence of water vapor excellent catalytic activity have been observed with the Pt loading of more than 0.5%. Even they reported that 100%

conversion of HCHO with the 0.1% platinum concentration. In the absence of moisture, conversion decrease to 8% with 0.1% of platinum loading. The result was confirming by the DRIFTs that formation of hydroxyl group in presence of humidity improves results. This leads to the conversion of HCHO in formate even absence of atmospheric oxygen. Zhao et al. (2012) has investigated the impact of water vapor on reaction stability and conversion of HCHO into CO_2 over MnO_x catalyst. Their report comes in the following form: for dryair flow approximate over 80% HCHO was converted into CO_2 by ozone and only 20% of CO_2 comes out. But for RH = 55%, ~oxidation of HCHO into CO_2 reported 100% with enhanced reaction stability. This conversion was supported by formation of O_3 which thoroughly oxidized HCHO into CO_2. A mechanistic study has been done by Huang et al. (2013b) for investigating the role of water vapor over Pd/TiO_2catalyst. They reported that 0.1% Pd made by deposition precipitation method shows strong activeness over HCHO decomposition and stable in the highly humid air. Analysis also include dissociated hydroxyl radical from water vapour support th process of adsorption and oxygen movement over the Pd/TiO_2 catalyst. They resulted that for RH = 50%, 100% HCHO conversion was observed while it was limited to 78.5 and 54.5% for 25% RH and 0% RH respectively.

3.4.2 Effect of calcination temperature

Calcination temperature plays an influencing role in catalytic oxidation of HCHO. Tang et al. (2006a) has synthesized MnO_x–CeO_2 catalyst at different calcinated temperature and resulted that below calcination temperature of 773 K due to making of MnO_x–CeO_2 solid solution. No diffraction peak related to manganese oxide has been observed and at the calcinated temperature of 773 K due to the phase isolation between MnO_2 and CeO_2, a clear diffraction peak observed for MnO_2.

3.4.3 Effect of preparation method

Preparation of catalyst for catalytic oxidation involves different processes such as Co-precipitation, impregnation, colloidal deposition method, microemulsion, sol–gel, and modified co-precipitation. An et al. (2013) has prepared a catalyst Pt/Fe_2O_3 for catalytic oxidation of HCHO using different methods which are co-precipitation, impregnation, and colloidal deposition methods which are listed in Table 2. Result shows that enhanced dispersion of Pt causes weakening of Fe–O bond at interface of Pt/FeO_x and hence improves the mobility of involved oxygen in oxidation of HCHO. Yu et al. (2011) have used high dispersion and small nano-sized Pt particles to improve the catalytic activity of $Pt/MnO_2$for HCHO oxidation using reflux the method and hydrothermal method which is also shown in Table 2. Tang et al. (2008) has used impregnation technique for preparation Pt/MnO_x–CeO_2 catalyst to decompose HCHO at room temperature. But An et al. (2013) has analyzed a different method to give a comparative view using co-precipitation (CP), impregnation (IMP), and colloidal deposition (CD). They resulted in higher catalytic activity for CD rather than CP and IMP method and proved through TEM result that at the surface of catalysts below 3 nm Pt particles were formed. Hence, it is clear that preparation method affects the structure of support and catalysts redox property. Tian et al. (2012) has used microemulsion process for birnessite type manganese oxides catalysts to increase the high surface area (upto 154 m^2/g).

3.4.4 Effect of feed rate of HCHO

The performance of catalytic oxidation of HCHO varied with fluctuation in feed rate of HCHO. The reaction rate of catalytic oxidation is much dependent on the molar ratio of oxygen to HCHO. Phenomena have been illustrated that lower the concentration ultimately decrease the light off temperature for catalytic oxidation of VOCs (Veser, Ziauddin, and Schmidt 1999). Peng and Wang (2007) has experiment the performance of noble metal catalyst with different feed rate of 100, 240, 400 mg/m^3 and resulted 41.5, 33.1, and 22.7% conversion at ambient temperature for HCHO respectively which is described in Table 2. This result ultimately illustrated that with the decrease in feed rate of HCHO would increase catalytic activity at ambient temperature. Reaction rate is generally not affected through mass transfer if fast mass transfer or very slow reaction rate happened. Similar results have been also illustrated by Tang et al. (2008) that excellent HCHO decomposition is getting through low concentration of HCHO. Kim, Park, and Hong (2011) has given a similar applicability of feed rate while catalytic oxidation of HCHO. They evaluated a proper applicability of feed rate that if reaction rate will increase with increase in HCHO inlet feed and vice versa. The trend observed that by increasing feed concentration there is decrement in overall catalytic activity. As temperature perspective Pei, Han, and Lu (2015) has evaluated the feed rate for catalytic oxidation of HCHO. They concluded that below 120 °C, decrease in conversion observed as inlet feed rate of HCHO increases and at ~180 °C the impact of inlet concentration of HCHO becomes obsolete. De la Peña O'Shea et al. (2005) has used two different feeds for the simultaneous decomposition of formaldehyde and methanol and result shows that different feeds have different 100% conversion temperature.

3.4.5 Effect of morphology

Morphology with exposed crystal plane on surface and crystallinity are crucial as a point of catalytic oxidation. Change in the morphology of oxide supported catalyst is in trend for regulating the catalytic activity (Feng et al. 2013; Zhou and Li 2012). Different morphology of gold doped ceria supported catalysts has been used. This involves nano-sized gold on finely defined CeO_2 nanorods in which deposition of gold demonstrated to weak the Ce–O bond by the clusters of gold. Due to creation of vacancy, O atom combines with Au atom at surface and this action would lead an electron to Ce by weaken CE–O bond (Xu et al. 2014a, 2014b). Lie et al. (Liu et al. 2012a) have used three-dimensionally averaged mesoporous Au/CeO_2 catalyst for improved catalysts supported by noble metal. They have observed that blockage of active sites on this structure may not happen with formed hydrocarbonate and carbonate. Hence this morphology shows efficient ways for oxidation of HCHO. 3D macroporous $Au/CeO_2–Co_3O_4$ catalyst with nanoporous walls (Liu et al. 2012b). Different morphological have been also used for MnO_2 for improvement in like pyrolusite, cryptomelane, and todorokite (de la Peña O'Shea et al. 2005). Co_3O_4 with 3D, 2D, and nanostructure possess a strong catalytic activity for abatement of HCHO (Bai, Arandiyan, and Li 2013). Su et al. (2019) have used cryptomelane type octahedral molecular sieve catalysts and investigated that degradation of HCHO on this morphology is greatly supported by reaction temperature from 50 to 110 °C.

3.4.6 Effect of support

For catalytic oxidation of HCHO large surface area is a prime requirement but this reactivity mainly influenced active component sites. Peng and Wang (2007) has compared the different supports $Ce_{0.8}Zr_{0.2}O_2$, $Ce_{0.2}Zr_{0.8}O_2$, SiO_2, and TiO_2 with 0.6 wt% loading of Pt for catalytic oxidation of HCHO and resulted that catalytic activity of TiO_2 based support is best among the SiO_2, $Ce_{0.2}Zr_{0.8}O_2$ and $Ce_{0.8}Zr_{0.2}O_2$ which is shown in Table 2 also. The degradation activity belongs to the well dispersion of Pt on different types of support. At the support because of small sized Pt, has a strong effect on degradation process. For evaluating the effect of support Park et al. (2012) has used different support of $Mn–CeO_2$, Al_2O_3, and TiO_2 with 0.25Pd/Beta zeolite catalyst for relative study at 50,000 h^{-1}. They resulted that 0.25 Pd/Beta and 0.25 Pd/Al_2O_3 catalysts could convert over 80% HCHO at 40 °C which illustrates that Beta Zeolite and Al_2O_3 come out as a strong catalyst as compare to TiO_2 and $Mn–CeO_2$ for low-temperature oxidation (below 100 °C). Yu et al. (2013) have used different support MnO_2/cotton possess strong catalytic activity for temperature below 100 °C. Graphene-based MnO_2 supported catalyst has been synthesized by Lu et al. (2016) and revealed that the graphene nanosheet just reduces the activation energy of MnO_2 catalyst from 85.5 and 39.5 kJ/mol.

3.4.7 Effect of metal addition to support

To enhance catalytic oxidation of HCHO over catalyst and improve the reaction rate this parameter also has been taken into consideration via different researchers. For example, Zhang et al. (2012) have used alkali addition to find the stronger catalytic activity for Pt/TiO_2catalyst at environment temperature and the effects are listed comprehensively in Table 2. These alkali metal ions (like K^+, Na^+, and Li^+) improve stability of catalysts by atomically dispersion. With different support of Pt/MnO_2, Chen et al. (2014) have examined the behavior of alkali metal salts for enhanced HCHO oxidation. The different salt used by Chen involves Na_2CO_3, Na_2SO_4, and $NaNO_3$ which resulted that at a lower temperature of 50 °C, 100% conversion of HCHO is getting through Na_2CO_3 additional catalysts. Similar tests have also been conducted on Pd/TiO_2 catalysts by modification of sodium by Zhang et al. (2014) with different loadings of sodium ion. They gave a comprehensive result that 2 wt% Na addition into Pd/TiO_2 converts 100% HCHO even at room temperature of 25 °C. The same results have been proposed by Li, Zhang, and He (2017) that due to addition 2 wt% Na catalytic surface produces abundant OH group which is ultimate increases the oxidation of HCHO.

4 Discussion on literature

In this paper, the methods of catalytic activation of HCHO at room temperature include two processes i.e. photocatalytic process and catalytic oxidation. With all the research main focus concentrated on photocatalyst and catalytic oxidation illustrated in this point of discussion. A photocatalytic oxidation process involves different processes during the decomposition of HCHO. These are: (1) flow of HCHO to the catalyst surface; (2) soaking of reactants on the catalyst surface; (3) irradiation of photon from light intensity; (4) redox reaction on catalyst surface; (5) flow of harmless product from surface, and (6) flow of product from the catalyst surface into the air. The important process in the PCO process is the absorption of the reactant, which have to oxidize. The adsorption process is an intermediate process which occurs before the photochemical reaction to start. So, adsorption of reactant is

important to concern while PCO. Another term that can enhance the activity of PCO is the selection of a proper reactor which extensively includes an annular reactor, monolith reactor, fluidized bed reactor, and powder plate reactor. The structures of photocatalysts also influence the PCO of HCHO. Nanoparticles with zero dimensionally have a high specific surface area, while 1D fiber tubes possess the advantage of light scattering properties. Various intermediate has also been observed during the photocatalytic oxidation of HCHO which are HCOOH, CO, Ozone, etc. and these species were quickly observed by catalyst surface. They would convert into CO_2 otherwise they will find as the outcome. The photocatalytic performance of titania can be enhanced by addition of metal and nonmetal which suppressed recombination of electron and hole pairs. Applicability of PCO had been limited to UV activation since it extended to the visible light range ($\lambda > 420$ nm) with the addition of proper doping.

There are many disadvantages of PCO listed here which are: (1) concentration of HCHO in the indoor environment is less, for that PCO doesn't show efficient performance due to high film diffusional resistance; (2) it is very difficult to increase the photocatalytic activity of reactor per unit volume since space limitation is there when doped through noble metal on TiO_2. As among all the noble metal catalysts and metal oxide catalysts, Pt shows good catalytic performance over oxidation of HCHO at room temperature. A small addition of Pt is enough for catalytic oxidation of formaldehyde but due to some limitation of high cost which makes Pt unused for practical application. Among various catalysts, Pd shows also good catalytic activity of different support like TiO_2, Al_2O_3, MnO_2, CeO_2, and Zeolite for the oxidation of HCHO and is abundantly available in nature. Negatively charged Pd supported catalysts improve the catalytic oxidation. For enhanced catalytic oxidation of HCHO with improved structure and chemical state, Pd species done well. With the proper support of metal oxide and with different morphology Pd catalysts can easily oxidize HCHO in CO_2, and H_2O at even room temperature. For lowering the temperature for catalytic oxidation addition of alkali plays an effective factor also. This effect is discussed in Table 2. Another noble metal, gold also does an influencing catalytic oxidation with well-defined morphology such as: three-dimensionally ordered macroporous with nanowalls.

There are some disadvantages noticed as well except the cost is poorly resistant to poisoning. Other than this, manganese oxide exhibits good catalytic properties to the different oxidation states available. Manganese and ceria oxide supports are well in oxygen storage capacity, redox properties, and thermal resistance. Different morphological changes like pyrolusite, cryptomelane, and todorokite in the case of MnO_x have a strong effect on reaction rate. The addition of noble metal over the transition metal oxide supported catalyst also improves the catalytic degradation of HCHO and makes the transition oxide catalysts preferable for the environmental temperature condition. The various structure has been used for enhancing the property of metal oxide such as CeO_2nanorods, graphene support MnO_x, manganese dioxide nano-sheets on cellulose fibers, nano-Co_3O_4, 3D-Co_3O_4 and 2D-Co_3O_4.

5 Conclusion

In this article, the most popular techniques for formaldehyde degradation i.e. photocatalytic oxidation and catalytic oxidation have been discussed. In spite of availability of efficient catalysts, the challenging work concern over higher efficiency, optimum design, and low cost availability. Moreover, the catalytic degradation of HCHO through the catalytic oxidation with noble metal and transitional metals supported metal oxide is emphasized in this review paper. To do this catalytic oxidation process subdivided into two main section; noble metal and metal oxide catalysts which give further insights the dependency of relative humidity, calcination temperature, preparation method, feed rate, morphology, addition of metal. In recent years a lot of work has been carried out on lowering temperature of oxidation of HCHO to room temperature with noble metal-supported metal oxide and transitional metal oxide.

In various articles, different groups have worked on nanostructures, reduction properties, active surface area, etc. So, the recent work corresponding to the degradation of indoor HCHO has been focused on designing and finding effective support like graphene, cotton, ZnO. Current work also just focused on varying operating parameters like preparation method, calcination temperature, the oxidation state of metals, etc. The addition of alkali, rare Earth metal to the supported catalyst is still not cleared with transition metal oxide. Other degradation processes like thermocatalytic process are also used but possess the difficulty of conversion of HCHO into CO_2 at ambient condition. Advanced processes are using this process with modification in morphology, concentration etc. to completely degrade the HCHO from the indoor environment. Element like MnO_2, without proper morphology and additives cannot enhance rate of degradation. The role of HCHO concentration, space velocity, and water vapor strongly affect the catalytic oxidation of HCHO. Long-time stability of catalyst and formation of the intermediate products are still a major concern for the practical application. In recent years, research work has been

concentrated on complete catalytic oxidation of HCHO at ambient temperature. Some works are really appreciable in this context. But there is still a large gap of their practical uses either due to cost or intermediate product limitation. However, the development of effective low-cost catalyst formation is the biggest work that has to be done. The work on transition metal oxides like (MnO_2, CeO_2) still needs a proper synthesis to work on room temperature of influencing the removal of formaldehyde.

Author contribution: All the authors have accepted responsibility for the entire content of this submitted manuscript and approved submission.
Research funding: None declared.
Conflict of interest statement: The authors declare no conflicts of interest regarding this article.

References

Adjimi, S., J. C. Roux, N. Sergent, F. Delpech, P. X. Thivel, and M. Pera-Titus. 2014. "Photocatalytic Oxidation of Ethanol Using Paper-Based Nano-TiO_2 Immobilized on Porous Silica: A Modelling Study." *Chemical Engineering Journal* 251: 381–91.

Akbarzadeh, R., S. B. Umbarkar, R. S. Sonawane, S. Takle, and M. K. Dongare. 2010. "Vanadia–Titania Thin Films for Photocatalytic Degradation of Formaldehyde in Sunlight." *Applied Catalysis A: General* 374 (1): 103–9.

Alexeev, O. S., S. Y. Chin, M. H. Engelhard, L. Ortiz-Soto, and M. D. Amiridis. 2005. "Effects of Reduction Temperature and Metal-Support Interactions on the Catalytic Activity of Pt/γ-Al_2O_3 and Pt/TiO_2 for the Oxidation of CO in the Presence and Absence of H_2." *The Journal of Physical Chemistry B* 109 (49): 23430–43.

Álvarez-Galván, M. C., B. Pawelec, V. A. De la Peña O'Shea, J. L. Fierro, and P. L. Arias. 2004. "Formaldehyde/Methanol Combustion on Alumina-Supported Manganese-Palladium Oxide Catalyst." *Applied Catalysis B: Environmental* 51 (2): 83–91.

An, N., Q. Yu, G. Liu, S. Li, M. Jia, and W. Zhang. 2011. "Complete Oxidation of Formaldehyde at Ambient Temperature over Supported Pt/Fe_2O_3 Catalysts Prepared by Colloid-Deposition Method." *Journal of Hazardous Materials* 186 (2): 1392–7.

An, N., P. Wu, S. Li, M. Jia, and W. Zhang. 2013. "Catalytic Oxidation of Formaldehyde over Pt/Fe_2O_3 Catalysts Prepared by Different Method." *Applied Surface Science* 285: 805–9.

Anpo, M., I. Tanahashi, and Y. Kubokawa. 1980. "Photoluminescence and Photoreduction of Vanadium Pentoxide Supported on Porous Vycor Glass." *The Journal of Physical Chemistry* 84 (25): 3440–3.

Anpo, M., N. Aikawa, Y. Kubokawa, M. Che, C. Louis, and E. Giamello. 1985. "Photoluminescence and Photocatalytic Activity of Highly Dispersed Titanium Oxide Anchored onto Porous Vycor Glass." *The Journal of Physical Chemistry* 89 (23): 5017–21.

Anpo, M., H. Yamashita, S. Kanai, K. Sato, T. Fujimoto, inventors, and Petroleum Energy Center, assignee 2000. "Photocatalyst, process for producing the photocatalyst, and photocatalytic reaction method." United States patent US 6,077,492. 2000.

Arzamendi, G., V. A. de la Peña O'Shea, M. C. Álvarez-Galván, J. L. Fierro, P. L. Arias, and L. M. Gandía. 2009. "Kinetics and Selectivity of Methyl–Ethyl–Ketone Combustion in Air over Alumina-Supported PdO_x–MnO_x Catalysts." *Journal of Catalysis* 261 (1): 50–9.

Asahi, R. Y., T. A. Morikawa, T. Ohwaki, K. Aoki, and Y. Taga. 2001. "Visible-Light Photocatalysis in Nitrogen-Doped Titanium Oxides." *Science* 293 (5528): 269–71.

Bai, B., and J. Li. 2014. "Positive Effects of K^+ Ions on Three-Dimensional Mesoporous Ag/Co_3O_4 Catalyst for HCHO Oxidation." *ACS Catalysis* 4 (8): 2753–62.

Bai, B., H. Arandiyan, and J. Li. 2013. "Comparison of the Performance for Oxidation of Formaldehyde on Nano-Co_3O_4, 2D-Co_3O_4, and 3D-Co_3O_4 Catalysts." *Applied Catalysis B: Environmental* 142: 677–83.

Benz, L., J. Haubrich, R. G. Quiller, S. C. Jensen, and C. M. Friend. 2009. "McMurry Chemistry on TiO_2 (110): Reductive C=C Coupling of Benzaldehyde Driven by Titanium Interstitials." *Journal of the American Chemical Society* 131 (41): 15026–31.

Bollinger, M. A., and M. A. Vannice. 1996. "A Kinetic and DRIFTS Study of Low-Temperature Carbon Monoxide Oxidation Over Au–TiO_2 Catalysts." *Applied Catalysis B: Environmental* 8 (4): 417–43.

Bowker, M., and R. A. Bennett. 2009. "The Role of Ti^{3+} Interstitials in TiO_2 (110) Reduction and Oxidation." *Journal of Physics: Condensed Matter* 21 (47): 474224.

Boyjoo, Y., H. Sun, J. Liu, V. K. Pareek, and S. Wang. 2017. "A Review on Photocatalysis for Air Treatment: from Catalyst Development to Reactor Design." *Chemical Engineering Journal* 310: 537–59.

Chen, H., J. He, C. Zhang, and H. He. 2007. "Self-Assembly of Novel Mesoporous Manganese Oxide Nanostructures and their Application in Oxidative Decomposition of Formaldehyde." *The Journal of Physical Chemistry C* 111 (49): 18033–8.

Chen, T., H. Dou, X. Li, X. Tang, J. Li, and J. Hao. 2009. "Tunnel Structure Effect of Manganese Oxides in Complete Oxidation of Formaldehyde." *Microporous and Mesoporous Materials* 122 (1): 270–4.

Chen, B. B., C. Shi, M. Crocker, Y. Wang, and A. M. Zhu. 2013. "Catalytic Removal of Formaldehyde at Room Temperature over Supported Gold Catalysts." *Applied Catalysis B: Environmental* 132: 245–55.

Chen, Y., J. He, H. Tian, D. Wang, and Q. Yang. 2014. "Enhanced Formaldehyde Oxidation on Pt/MnO_2 Catalysts Modified with Alkali Metal Salts." *Journal of Colloid and Interface Science* 428: 1–7.

Cordi, E. M., and J. L. Falconer. 1996. "Oxidation of Volatile Organic Compounds on Al_2O_3, Pd/Al_2O_3, and PdO/Al_2O_3 Catalysts." *Journal of Catalysis* 162 (1): 104–17.

de la Peña O'Shea, V. A., M. C. Alvarez-Galvan, J. L. Fierro, and P. L. Arias. 2005. "Influence of Feed Composition on the Activity of Mn and PdMn/Al_2O_3 Catalysts for Combustion of Formaldehyde/Methanol." *Applied Catalysis B: Environmental* 57 (3): 191–9.

Delannoy, L., K. Fajerwerg, P. Lakshmanan, C. Potvin, C. Méthivier, and C. Louis. 2010. "Supported Gold Catalysts for the Decomposition of VOC: Total Oxidation of Propene in Low Concentration as Model Reaction." *Applied Catalysis B: Environmental* 94 (1): 117–24.

Deng, X. Q., J. L. Liu, X. S. Li, B. Zhu, X. Zhu, and A. M. Zhu. 2017. "Kinetic Study on Visible-Light Photocatalytic Removal of

Formaldehyde from Air over Plasmonic Au/TiO_2." *Catalysis Today* 281: 630–5.

Ding, H. X., A. M. Zhu, F. G. Lu, Y. Xu, J. Zhang, and X. F. Yang. 2006. "Low-temperature Plasma-Catalytic Oxidation of Formaldehyde in Atmospheric Pressure Gas Streams." *Journal of Physics D: Applied Physics* 39 (16): 3603.

Dobrosz-Gómez, I., I. Kocemba, and J. M. Rynkowski. 2008. "Au/$Ce_{1-x}Zr_xO_2$ as Effective Catalysts for Low-Temperature CO Oxidation." *Applied Catalysis B: Environmental* 83 (3): 240–55.

Domingo-Garcia, M., I. Fernández-Morales, F. J. Lopez-Garzon, C. Moreno-Castilla, and M. Perez-Mendoza. 1999. "On the Adsorption of Formaldehyde at High Temperatures and Zero Surface Coverage." *Langmuir* 15 (9): 3226–31.

Feng, Y., I. S. Cho, L. Cai, P. M. Rao, and X. Zheng. 2013. "Sol-Flame Synthesis of Hybrid Metal Oxide Nanowires." *Proceedings of the Combustion Institute* 34 (2): 2179–86.

Fu, P., P. Zhang, and J. Li. 2011. "Photocatalytic Degradation of Low Concentration Formaldehyde and Simultaneous Elimination of Ozone By-product using Palladium Modified TiO2 Films Under UV254+ 185nm irradiation." *Applied Catalysis B: Environmental* 105: 220.

Gluhoi, A. C., N. Bogdanchikova, and B. E. Nieuwenhuys. 2005. "The Effect of Different Types of Additives on the Catalytic Activity of Au/Al_2O_3 in Propene Total Oxidation: Transition Metal Oxides and Ceria." *Journal of Catalysis* 229 (1): 154–62.

Goode, J. W. 1985. "Toxicology of Formaldehyde." *Advances in Chemistry* 210: 217–27.

Goswami, D. Y. 1998. "Photocatalytic System for Indoor Air Quality," US Patent Serial No. 5,835,840, November 10, 1998.

Goswami, D. Y. 1999a. "Photocatalytic Air Disinfection." U.S. Patent Serial No. 5,933,702 August 3, 1999.

Goswami, D. Y. 1999b. "Electrostatic Photocatalytic Air Disinfection," U.S. Patent Serial No. 5,993,738, November 30, 1999.

Goswami, D. Y. 2003. "Decontamination of Ventilation Systems Using Photocatalytic Air Cleaning Technology." *Journal of Solar Energy Engineering* 125 (3): 359–65.

Goswami, D. Y. 2008. "Enhanced Photocatalytic Air Detoxification and Disinfection by Active Electron Transfer." US Patent No 7,371,351, May 13, 2008.

Goswami, D. Y., D. M. Trivedi, and S. S. Block. 1997. "Photocatalytic Disinfection of Indoor Air." *Journal of Solar Energy Engineering* 119 (1): 92–6.

Groppi, G., and E. Tronconi. 2005. "Honeycomb Supports with High Thermal Conductivity for Gas/solid Chemical Processes." *Catalysis Today* 105 (3): 297–304.

Gupta, J., K. C. Barick, and D. Bahadur. 2011. "Defect Mediated Photocatalytic Activity in Shape-Controlled ZnO Nanostructures." *Journal of Alloys and Compounds* 509 (23): 6725–30.

Haruta, M., N. Yamada, T. Kobayashi, and S. Iijima. 1989. "Gold Catalysts Prepared by Coprecipitation for Low-Temperature Oxidation of Hydrogen and of Carbon Monoxide." *Journal of Catalysis* 115 (2): 301–9.

Hashimoto, K., H. Irie, and A. Fujishima. 2005. "TiO_2 Photocatalysis Historical Overview and Future Prospect." *Japanese Journal of Applied Physics. Part 1* 44 (12): 8269–85.

Hoffmann, M. R., S. T. Martin, W. Choi, and D. W. Bahnemann. 1995. "Environmental Applications of Semiconductor Photocatalysis." *Chemical Reviews* 95 (1): 69–96.

Hong, Y. C., K. Q. Sun, K. H. Han, G. Liu, and B. Q. Xu. 2010. "Comparison of Catalytic Combustion of Carbon Monoxide and Formaldehyde over Au/ZrO_2 Catalysts." *Catalysis Today* 158 (3): 415–22.

Hosseini, M., T. Barakat, R. Cousin, A. Aboukaïs, B. L. Su, G. De Weireld, and S. Siffert. 2012. "Catalytic Performance of Core–Shell and Alloy Pd–Au Nanoparticles for Total Oxidation of VOC: The Effect of Metal Deposition." *Applied Catalysis B: Environmental* 111: 218–24.

Hu, P., Z. Amghouz, Z. Huang, F. Xu, Y. Chen, and X. Tang. 2015. "Surface-confined Atomic Silver Centers Catalyzing Formaldehyde Oxidation." *Environmental Science & Technology* 49 (4): 2384–90.

Huang, H., and D. Y. Leung. 2011a. "Complete Oxidation of Formaldehyde at Room Temperature Using TiO_2 Supported Metallic Pd Nanoparticles." *ACS Catalysis* 1 (4): 348–54.

Huang, H., and D. Y. Leung. 2011b. "Complete Elimination of Indoor Formaldehyde Over Supported Pt Catalysts with Extremely Low Pt Content at Ambient Temperature." *Journal of Catalysis* 280 (1): 60–7.

Huang, H., X. Ye, H. Huang, L. Zhang, and D. Y. Leung. 2013a. "Mechanistic Study on Formaldehyde Removal over Pd/TiO_2 Catalysts: Oxygen Transfer and Role of Water Vapor." *Chemical Engineering Journal* 230: 73–9.

Huang, Q., W. Ma, X. Yan, Y. Chen, S. Zhu, and S. Shen. 2013b. "Photocatalytic Decomposition of Gaseous HCHO by $Zr_xTi_{1-x}O_2$ Catalysts under UV–Vis Light Irradiation with an Energy-Saving Lamp." *Journal of Molecular Catalysis A: Chemical* 366: 261–5.

Ibhadon, A. O., I. M. Arabatzis, P. Falaras, and D. Tsoukleris. 2007. "The Design and Photoreaction Kinetic Modeling of a Gas-Phase Titania Foam Packed Bed Reactor." *Chemical Engineering Journal* 133 (1–3): 317–23.

Imamura, S., Y. Uematsu, K. Utani, and T. Ito. 1991. "Combustion of Formaldehyde on Ruthenium/cerium (IV) Oxide Catalyst." *Industrial & Engineering Chemistry Research* 30 (1): 18–21.

Imamura, S., D. Uchihori, K. Utani, and T. Ito. 1994. "Oxidative Decomposition of Formaldehyde on Silver-Cerium Composite Oxide Catalyst." *Catalysis Letters* 24 (3): 377–84.

Jin, M., X. Zhang, S. Nishimoto, Z. Liu, D. A. Tryk, A. V. Emeline, T. Murakami, and A. Fujishima. 2007. "Light-stimulated Composition Conversion in TiO_2-Based Nanofibers." *The Journal of Physical Chemistry C* 111 (2): 658–65.

Kecskés, T., J. Raskó, and J. Kiss. 2004. "FTIR and Mass Spectrometric Studies on the Interaction of Formaldehyde with TiO_2 Supported Pt and Au Catalysts." *Applied Catalysis A: General* 273 (1): 55–62.

Khan, S. U., M. Al-Shahry, and W. B. Ingler. 2002. "Efficient photochemical water splitting by a chemically modified *n*-TiO_2." *Science* 297 (5590): 2243–5.

Kim, S. S., K. H. Park, and S. C. Hong. 2011. "A Study on HCHO Oxidation Characteristics at Room Temperature Using a Pt/TiO_2 Catalyst." *Applied Catalysis A: General* 398 (1): 96–103.

Kocareva, T., I. Grozdanov, and B. Pejova. 2001. "Ag and AgO Thin Film Formation in Ag^+-Triethanolamine Solutions." *Materials Letters* 47 (6): 319–23.

Kołodziej, A., and J. Łojewska. 2005. "Optimization of Structured Catalyst Carriers for VOC Combustion." *Catalysis Today* 105 (3): 378–84.

Kwon, D. W., P. W. Seo, G. J. Kim, and S. C. Hong. 2015. "Characteristics of the HCHO Oxidation Reaction over Pt/TiO_2

Catalysts at Room Temperature: The Effect of Relative Humidity on Catalytic Activity." *Applied Catalysis B: Environmental* 163: 436–43.

Lam, R. C., M. K. Leung, D. Y. Leung, L. L. Vrijmoed, W. C. Yam, and S. P. Ng. 2007. "Visible-Light-Assisted Photocatalytic Degradation of Gaseous Formaldehyde by Parallel-Plate Reactor Coated with Cr Ion-Implanted TiO_2 Thin Film." *Solar Energy Materials and Solar Cells* 91 (1): 54–61.

Landis, E. C., S. C. Jensen, K. R. Phillips, and C. M. Friend. 2012. "Photostability and Thermal Decomposition of Benzoic Acid on TiO_2." *The Journal of Physical Chemistry C* 116 (40): 21508–13.

Li, S. C., and U. Diebold. 2009. "Reactivity of TiO_2 Rutile and Anatase Surfaces toward Nitroaromatics." *Journal of the American Chemical Society* 132 (1): 64–6.

Li, C. Y., Y. N. Shen, R. S. Hu, P. P. Li, and J. Zhang. 2007. "Catalytic Activity of Au/Fe-PILC and Au/Fe-Oxide Catalysts for Catalytic Combustion of Formaldehyde." *Transactions of Nonferrous Metals Society of China* 17 (s1B): s1107–11.

Li, C., Y. Shen, M. Jia, S. Sheng, M. O. Adebajo, and H. Zhu. 2008. "Catalytic Combustion of Formaldehyde on Gold/Iron-Oxide Catalysts." *Catalysis Communications* 9 (3): 355–61.

Li, Y., Y. Jiang, S. Peng, and F. Jiang. 2010. "Nitrogen-doped TiO_2 Modified with NH_4F for Efficient Photocatalytic Degradation of Formaldehyde under Blue Light-Emitting Diodes." *Journal of Hazardous Materials* 182 (1): 90–6.

Li, H. F., N. Zhang, P. Chen, M. F. Luo, and J. Q. Lu. 2011. "High Surface Area Au/CeO_2 Catalysts for Low Temperature Formaldehyde Oxidation." *Applied Catalysis B: Environmental* 110: 279–85.

Li, J. W., K. L. Pan, S. J. Yu, S. Y. Yan, and M. B. Chang. 2014. "Removal of Formaldehyde over $Mn_xCe_{1-x}O_2$ Catalysts: Thermal Catalytic Oxidation Versus Ozone Catalytic Oxidation." *Journal of Environmental Sciences* 26 (12): 2546–53.

Li, D., G. Yang, P. Li, J. Wang, and P. Zhang. 2016a. "Promotion of Formaldehyde Oxidation over Ag Catalyst by Fe Doped MnO_X Support at Room Temperature." *Catalysis Today* 277: 257–65.

Li, Y., C. Zhang, H. He, J. Zhang, and M. Chen. 2016b. "Influence of Alkali Metals on Pd/TiO_2 Catalysts for Catalytic Oxidation of Formaldehyde at Room Temperature." *Catalysis Science & Technology* 6 (7): 2289–95.

Li, Y., C. Zhang, and H. He. 2017. "Significant Enhancement in Activity of Pd/TiO_2 Catalyst for Formaldehyde Oxidation by Na Addition." *Catalysis Today* 281: 412–7.

Liang, W. J., J. Li, J. X. Li, T. Zhu, and Y. Q. Jin. 2010. "Formaldehyde Removal from Gas Streams by Means of $NaNO_2$ Dielectric Barrier Discharge Plasma." *Journal of Hazardous Materials* 175 (1): 1090–5.

Liang, W., J. Li, and Y. Jin. 2012. "Photo-catalytic Degradation of Gaseous Formaldehyde by TiO_2/UV, Ag/TiO_2/UV and Ce/TiO_2/UV." *Building and Environment* 51: 345–50.

Liao, Y., C. Xie, Y. Liu, and Q. Huang. 2013. "Enhancement of Photocatalytic Property of ZnO for Gaseous Formaldehyde Degradation by Modifying Morphology and Crystal Defect." *Journal of Alloys and Compounds* 550: 190–7.

Lin, L., W. Lin, J. L. Xie, Y. X. Zhu, B. Y. Zhao, and Y. C. Xie. 2007. "Photocatalytic Properties of Phosphor-Doped Titania Nanoparticles." *Applied Catalysis B: Environmental* 75 (1): 52–8.

Liotta, L. F. 2010. "Catalytic Oxidation of Volatile Organic Compounds on Supported Noble Metals." *Applied Catalysis B: Environmental* 100 (3): 403–12.

Liu, S. H., and W. X. Lin. 2019. "A Simple Method to Prepare G-C_3N_4-TiO_2/Waste Zeolites as Visible-Light-Responsive Photocatalytic Coatings for Degradation of Indoor Formaldehyde." *Journal of Hazardous Materials* 15 (368): 468–76.

Liu, Y., C. Y. Liu, Q. H. Rong, and Z. Zhang. 2003. "Characteristics of the Silver-Doped TiO_2 Nanoparticles." *Applied Surface Science* 220 (1): 7–11.

Liu, H. Y., X. J. Wang, L. P. Wang, F. Y. Lei, X. F. Wang, and H. J. Ai. 2008. "Effect of Fluoride-Ion Implantation on the Biocompatibility of Titanium for Dental Applications." *Applied Surface Science* 254 (20): 6305–12.

Liu, L., H. Tian, J. He, D. Wang, and Q. Yang. 2012a. "Preparation of Birnessite-Supported Pt Nanoparticles and their Application in Catalytic Oxidation of Formaldehyde." *Journal of Environmental Sciences* 24 (6): 1117–24.

Liu, B., C. Li, Y. Zhang, Y. Liu, W. Hu, Q. Wang, L. Han, and J. Zhang. 2012b. "Investigation of Catalytic Mechanism of Formaldehyde Oxidation over Three-Dimensionally Ordered Macroporous Au/CeO_2 Catalyst." *Applied Catalysis B: Environmental* 111: 467–75.

Liu, B., Y. Liu, C. Li, W. Hu, P. Jing, Q. Wang, and J. Zhang. 2012c. "Three-dimensionally Ordered Macroporous Au/CeO_2–Co_3O_4 Catalysts with Nanoporous Walls for Enhanced Catalytic Oxidation of Formaldehyde." *Applied Catalysis B: Environmental* 127: 47–58.

Lu, G., A. Linsebigler, and J. T. Yates Jr. 1994. "Ti^{3+} Defect Sites on TiO_2 (110): Production and Chemical Detection of Active Sites." *The Journal of Physical Chemistry* 98 (45): 11733–8.

Lu, L., H. Tian, J. He, and Q. Yang. 2016. "Graphene–MnO_2 Hybrid Nanostructure as a New Catalyst for Formaldehyde Oxidation." *The Journal of Physical Chemistry C* 120 (41): 23660–8.

Ma, C., D. Wang, W. Xue, B. Dou, H. Wang, and Z. Hao. 2011. "Investigation of Formaldehyde Oxidation over Co_3O_4–CeO_2 and Au/Co_3O_4–CeO_2 Catalysts at Room Temperature: Effective Removal and Determination of Reaction Mechanism." *Environmental Science & Technology* 45 (8): 3628–34.

Ma, L., D. Wang, J. Li, B. Bai, L. Fu, and Y. Li. 2014. "Ag/CeO_2 Nanospheres: Efficient Catalysts for Formaldehyde Oxidation." *Applied Catalysis B: Environmental* 148: 36–43.

Matsuo, Y., Y. Nishino, T. Fukutsuka, and Y. Sugie. 2008. "Removal of Formaldehyde from Gas Phase by Silylated Graphite Oxide Containing Amino Groups." *Carbon* 46 (8): 1162–3.

Mirkelamoglu, B., and G. Karakas. 2006. "The Role of Alkali-Metal Promotion on CO Oxidation over PdO/SnO_2 Catalysts." *Applied Catalysis A: General* 299: 84–94.

Nie, L., J. Yu, X. Li, B. Cheng, G. Liu, and M. Jaroniec. 2013. "Enhanced Performance of NaOH-Modified Pt/TiO_2 toward Room Temperature Selective Oxidation of Formaldehyde." *Environmental Science & Technology* 47 (6): 2777–83.

Noguchi, T., A. Fujishima, P. Sawunyama, and K. Hashimoto. 1998. "Photocatalytic Degradation of Gaseous Formaldehyde Using TiO_2 Film." *Environmental Science & Technology* 32 (23): 3831–3.

Norbäck, D., C. Edling, and G. Wieslander. 1994. "Asthma Symptoms and the Sick Building Syndrome (SBS)—The Significance of Microorganisms in the Indoor Environment. Health Implications of Fungi in Indoor Environments." *Air Quality Monographs* 2: 229–39.

Ohno, T., M. Akiyoshi, T. Umebayashi, K. Asai, T. Mitsui, and M. Matsumura. 2004. "Preparation of S-doped TiO_2 photocatalysts and their photocatalytic activities under visible light." *Applied Catalysis A: General* 265 (1): 115–21.

Ohtani, B. 2008. "Preparing Articles on Photocatalysis—Beyond the Illusions, Misconceptions, and Speculation." *Chemistry Letters* 37 (3): 216–29.

Ollis, D. F. 2000. "Photocatalytic purification and remediation of contaminated air and water." *Comptes Rendus de l'Académie des Sciences-Series IIC-Chemistry* 3 (6): 405–11.

Ordóñez, S., L. Bello, H. Sastre, R. Rosal, and F. V. Díez. 2002. "Kinetics of the Deep Oxidation of Benzene, Toluene, N-Hexane and their Binary Mixtures over a Platinum on γ-Alumina Catalyst." *Applied Catalysis B: Environmental* 38 (2): 139–49.

Park, S. J., I. Bae, I. S. Nam, B. K. Cho, S. M. Jung, and J. H. Lee. 2012. "Oxidation of Formaldehyde over Pd/Beta Catalyst." *Chemical Engineering Journal* 195: 392–402.

Passalía, C., O. M. Alfano, and R. J. Brandi. 2012. "A Methodology for Modeling Photocatalytic Reactors for Indoor Pollution Control Using Previously Estimated Kinetic Parameters." *Journal of Hazardous Materials* 211: 357–65.

Pei, J., and J. S. Zhang. 2011. "Critical Review of Catalytic Oxidization and Chemisorption Methods for Indoor Formaldehyde Removal." *HVAC & R Research* 17 (4): 476–503.

Pei, J., X. Han, and Y. Lu. 2015. "Performance and Kinetics of Catalytic Oxidation of Formaldehyde over Copper Manganese Oxide Catalyst." *Building and Environment* 84: 134–41.

Peng, J., and S. Wang. 2007. "Performance and Characterization of Supported Metal Catalysts for Complete Oxidation of Formaldehyde at Low Temperatures." *Applied Catalysis B: Environmental* 73 (3–4): 282–91.

Photong, S., and V. Boonamnuayvitaya. 2009. "Preparation and Characterization of Amine-Functionalized SiO_2/TiO_2 Films for Formaldehyde Degradation." *Applied Surface Science* 255 (23): 9311–5.

Popova, M., Á. Szegedi, Z. Cherkezova-Zheleva, A. Dimitrova, and I. Mitov. 2010. "Toluene Oxidation on Chromium- and Copper-Modified SiO_2 and SBA-15." *Applied Catalysis A: General* 381 (1): 26–35.

Qin, Y., Z. Wang, J. Jiang, L. Xing, and K. Wu. 2020. "One-step Fabrication of TiO_2/Ti Foil Annular Photoreactor for Photocatalytic Degradation of Formaldehyde." *Chemical Engineering Journal*: 124917. https://doi.org/10.1016/j.cej.2020.124917.

Reed, J., and G. Ceder. 2004. "Role of Electronic Structure in the Susceptibility of Metastable Transition-Metal Oxide Structures to Transformation." *Chemical Reviews* 104 (10): 4513–34.

Scire, S., S. Minico, C. Crisafulli, C. Satriano, and A. Pistone. 2003. "Catalytic Combustion of Volatile Organic Compounds on Gold/cerium Oxide Catalysts." *Applied Catalysis B: Environmental* 40 (1): 43–9.

Sekine, Y. 2002. "Oxidative Decomposition of Formaldehyde by Metal Oxides at Room Temperature." *Atmospheric Environment* 36 (35): 5543–7.

Serre, C., F. Garin, G. Belot, and G. Maire. 1993. "Reactivity of Pt/Al_2O_3 and $Pt\text{-}CeO_2Al_2O_3$ Catalysts for the Oxidation of Carbon Monoxide by Oxygen: II. Influence of the Pretreatment Step on the Oxidation Mechanism." *Journal of Catalysis* 141 (1): 9–20.

Shi, J., H. N. Cui, Z. Liang, X. Lu, Y. Tong, C. Su, and H. Liu. 2011. "The Roles of Defect States in Photoelectric and Photocatalytic Processes for $Zn_xCd_{1-x}S$." *Energy & Environmental Science* 4 (2): 466–70.

Shi, C., Y. Wang, A. Zhu, B. Chen, and C. Au. 2012a. "$Mn_XCo_{3-X}O_4$ Solid Solution as High-Efficient Catalysts for Low-Temperature Oxidation of Formaldehyde." *Catalysis Communications* 28: 18–22.

Shi, C., B. B. Chen, X. S. Li, M. Crocker, Y. Wang, and A. M. Zhu. 2012b. "Catalytic Formaldehyde Removal by "Storage-oxidation" Cycling Process over Supported Silver Catalysts." *Chemical Engineering Journal* 200: 729–37.

Singh, P., and S. R. Chauhan. 2016. "Carbonyl and Aromatic Hydrocarbon Emissions from Diesel Engine Exhaust Using Different Feedstock: A Review." *Renewable and Sustainable Energy Reviews* 63: 269–91.

Sinha, A. K., K. Suzuki, M. Takahara, H. Azuma, T. Nonaka, N. Suzuki, and N. Takahashi. 2008. "Preparation and Characterization of Mesostructured γ-manganese Oxide and its Application to VOCs Elimination." *The Journal of Physical Chemistry C* 112 (41): 16028–35.

Skrobot, F. C., A. A. Valente, G. Neves, I. Rosa, J. Rocha, and J. A. S. Cavaleiro. 2003. "Monoterpenes Oxidation in the Presence of Y Zeolite-Entrapped Manganese (III) Tetra (4-N-benzylpyridyl) Porphyrin." *Journal of Molecular Catalysis A: Chemical* 201: 211.

Su, J., C. Cheng, Y. Guo, H. Xu, and Q. Ke. 2019. "OMS-2-Based Catalysts with Controllable Hierarchical Morphologies for Highly Efficient Catalytic Oxidation of Formaldehyde." *Journal of Hazardous Materials* 15 (380): 120890.

Tan, H., J. Wang, S. Yu, and K. Zhou. 2015. "Support Morphology-Dependent Catalytic Activity of Pd/CeO_2 for Formaldehyde Oxidation." *Environmental Science & Technology* 49 (14): 8675–82.

Tang, X., J. Chen, Y. Li, Y. Li, Y. Xu, and W. Shen. 2006a. "Complete Oxidation of Formaldehyde over Ag/MnO_x–CeO_2 Catalysts." *Chemical Engineering Journal* 118 (1–2): 119–25.

Tang, X., Y. Li, X. Huang, Y. Xu, H. Zhu, J. Wang, and W. Shen. 2006b. "MnO_x–CeO_2 Mixed Oxide Catalysts for Complete Oxidation of Formaldehyde: Effect of Preparation Method and Calcination Temperature." *Applied Catalysis B: Environmental* 62 (3): 265–73.

Tang, X., J. Chen, X. Huang, Y. Xu, and W. Shen. 2008. "Pt/MnO_x–CeO_2 Catalysts for the Complete Oxidation of Formaldehyde at Ambient Temperature." *Applied Catalysis B: Environmental* 81 (1): 115–21.

Terelak, K., S. Trybula, M. Majchrzak, M. Ott, and H. Hasse. 2005. "Pilot Plant Formaldehyde Distillation: Experiments and Modelling." *Chemical Engineering and Processing: Process Intensification* 44 (6): 671–6.

Tian, H., J. He, L. Liu, D. Wang, Z. Hao, and C. Ma. 2012. "Highly Active Manganese Oxide Catalysts for Low-Temperature Oxidation of Formaldehyde." *Microporous and Mesoporous Materials* 151: 397–402.

Tompkins D. T. 2001. "Evaluation of Photocatalytic Air Cleaning Capability: a Literature Review and Engineering Analysis." ASHARE Research Project RP-1134.

Tsukamoto, D., Y. Shiraishi, Y. Sugano, S. Ichikawa, S. Tanaka, and T. Hirai. 2012. "Gold Nanoparticles Located at the Interface of Anatase/Rutile TiO_2 Particles as Active Plasmonic Photocatalysts for Aerobic Oxidation." *Journal of the American Chemical Society* 134 (14): 6309–15.

Ubolchonlakate, K., L. Sikong, and T. Tontai. 2010. "Formaldehyde Degradation by Photocatalytic Ag-Doped TiO_2 Film of Glass Fiber Roving." *Journal of Nanoscience and Nanotechnology* 10 (11): 7522–5.

Venkataraj, S., O. Kappertz, R. Drese, C. Liesch, R. Jayavel, and M. Wuttig. 2002. "Thermal Stability of Lead Oxide Films Prepared by Reactive DC Magnetron Sputtering." *Physica Status Solidi (a)* 194 (1): 192–205.

Veser, G., M. Ziauddin, and L. D. Schmidt. 1999. "Ignition in Alkane Oxidation on Noble-Metal Catalysts." *Catalysis Today* 47 (1): 219–28.

Vijayakrishnan, V., A. Chainani, D. D. Sarma, and C. N. Rao. 1992. "Metal-insulator Transitions in Metal Clusters: A High-Energy Spectroscopy Study of Palladium and Silver Clusters." *The Journal of Physical Chemistry* 96 (22): 8679–82.

Villegas, J. C., L. J. Garces, S. Gomez, J. P. Durand, and S. L. Suib. 2005. "Particle Size Control of Cryptomelanenanomaterials by Use of H_2O_2 in Acidic Conditions." *Chemistry of Materials* 17 (7): 1910–8.

Vohra, A., D. Y. Goswami, D. A. Deshpande, and S. S. Block. 2005. "Enhanced Photocatalytic Inactivation of Bacterial Spores on Surfaces in Air." *Journal of Industrial Microbiology and Biotechnology* 32 (8): 364.

Vohra, A., D. Y. Goswami, D. A. Deshpande, and S. S. Block. 2006. "Enhanced Photocatalytic Disinfection of Indoor Air." *Applied Catalysis B: Environmental* 64 (1–2): 57–65.

Wang, C., and D. Astruc. 2014. "Nano Gold Plasmonic Photocatalysis for Organic Synthesis and Clean Energy Conversion." *Chemical Society Reviews* 43 (20): 7188–216.

Wang, R., and J. Li. 2009. "OMS-2 Catalysts for Formaldehyde Oxidation: Effects of Ce and Pt on Structure and Performance of the Catalysts." *Catalysis Letters* 131 (3–4): 500–5.

Wang, R., and J. Li. 2010. "Effects of Precursor and Sulfation on OMS-2 Catalyst for Oxidation of Ethanol and Acetaldehyde at Low Temperatures." *Environmental Science & Technology* 44 (11): 4282–7.

Wang, Q., J. Biener, X. C. Guo, E. Farfan-Arribas, and R. J. Madix. 2003. "Reactivity of Stoichiometric and Defective TiO_2 (110) Surfaces toward DCOOD Decomposition." *The Journal of Physical Chemistry B* 107 (42): 11709–20.

Wang, X., J. C. Yu, Y. Chen, L. Wu, and X. Fu. 2006. "ZrO_2-Modified MesoporousNanocrystalline $TiO_{2-x}N_x$ as Efficient Visible Light Photocatalysts." *Environmental Science & Technology* 40 (7): 2369–74.

Wang, S., H. M. Ang, and M. O. Tade. 2007. "Volatile Organic Compounds in Indoor Environment and Photocatalytic Oxidation: State of the Art." *Environment International* 33 (5): 694–705.

Wang, M. M., L. He, Y. M. Liu, Y. Cao, H. Y. He, and K. N. Fan. 2011. "Gold Supported on Mesostructured Ceria as an Efficient Catalyst for the Chemoselective Hydrogenation of Carbonyl Compounds in Neat Water." *Green Chemistry* 13 (3): 602–7.

Wang, B., X. Wu, R. Ran, Z. Si, and D. Weng. 2012. "Participation of Sulfates in Propane Oxidation on $Pt/SO_4^{2-}/CeO^{2-}$ ZrO_2 Catalyst." *Journal of Molecular Catalysis A: Chemical* 361: 98–103.

Wen, Y., X. Tang, J. Li, J. Hao, L. Wei, and X. Tang. 2009. "Impact of Synthesis Method on Catalytic Performance of MnO_x–SnO_2 for Controlling Formaldehyde Emission." *Catalysis Communications* 10 (8): 1157–60.

Wu, P. C., Y. Y. Li, C. C. Lee, C. M. Chiang, and H. J. Su. 2003. "Risk Assessment of Formaldehyde in Typical Office Buildings in Taiwan." *Indoor Air* 13 (4): 359–63.

Xingfu, T., X. Huang, S. Jianjun, L. I. Junlong, L. I. Yonggang, X. U. Yide, and S. H. Wenjie. 2006. "Synthesis and Catalytic Performance of Manganese Oxide Octahedral Molecular Sieve Nanorods for Formaldehyde Oxidation at Low Temperature." *Chinese Journal of Catalysis* 27 (2): 97–9.

Xu, Y., and M. A. Schoonen. 2000. "The Absolute Energy Positions of Conduction and Valence Bands of Selected Semiconducting Minerals." *American Mineralogist* 85 (3–4): 543–56.

Xu, Z., N. Qin, J. Wang, and H. Tong. 2010. "Formaldehyde Biofiltration as Affected by Spider Plant." *Bioresource Technology* 101 (18): 6930–4.

Xu, Q., Y. Zhang, J. Mo, and X. Li. 2011. "Indoor Formaldehyde Removal by Thermal Catalyst: Kinetic Characteristics, Key Parameters, and Temperature Influence." *Environmental Science & Technology* 45 (13): 5754–60.

Xu, Q., W. Lei, X. Li, X. Qi, J. Yu, G. Liu, J. Wang, and P. Zhang. 2014a. "Efficient Removal of Formaldehyde by Nanosized Gold on Well-Defined CeO_2 Nanorods at Room Temperature." *Environmental Science & Technology* 48 (16): 9702–8.

Xu, Q., W. Lei, X. Li, X. Qi, J. Yu, G. Liu, J. Wang, and P. Zhang. 2014b. "Efficient Removal of Formaldehyde by Nanosized Gold on Well-Defined CeO_2 Nanorods at Room Temperature." *Environmental Science & Technology* 48 (16): 9702–8.

Yamashita, H., M. Honda, M. Harada, Y. Ichihashi, M. Anpo, T. Hirao, N. Itoh, and N. Iwamoto. 1998. "Preparation of Titanium Oxide Photocatalysts Anchored on Porous Silica Glass by a Metal Ion-Implantation Method and Their Photocatalytic Reactivities for the Degradation of 2-propanol Diluted in Water." *The Journal of Physical Chemistry B* 102 (52): 10707–11.

Yang, L., and Z. Liu. 2007. "Study on Light Intensity in the Process of Photocatalytic Degradation of Indoor Gaseous Formaldehyde for Saving Energy." *Energy Conversion and Management* 48 (3): 882–9.

Yang, J., D. Li, Z. Zhang, Q. Li, and H. Wang. 2000. "A Study of the Photocatalytic Oxidation of Formaldehyde on $Pt/Fe_2O_3/TiO_2$." *Journal of Photochemistry and Photobiology A: Chemistry* 137 (2): 197–202.

Yang, S., W. Zhu, Z. Jiang, Z. Chen, and J. Wang. 2006. "The Surface Properties and the Activities in Catalytic Wet Air Oxidation over CeO_2–TiO_2 Catalysts." *Applied Surface Science* 252 (24): 8499–505.

Yang, L., Z. Liu, J. Shi, Y. Zhang, H. Hu, and W. Shangguan. 2007. "Degradation of Indoor Gaseous Formaldehyde by Hybrid VUV and TiO_2/UV Processes." *Separation and Purification Technology* 54 (2): 204–11.

Yang, K., J. Liu, R. Si, X. Chen, W. Dai, and X. Fu. 2014. "Comparative Study of Au/TiO_2 and Au/Al_2O_3 for Oxidizing CO in the Presence of H2 under Visible Light Irradiation." *Journal of Catalysis* 317: 229–39.

Yentekakis, I. V., G. Moggridge, C. G. Vayenas, and R. M. Lambert. 1994. "In Situ controlled Promotion of Catalyst Surfaces via NEMCA: The Effect of Na on the Pt-Catalyzed CO Oxidation." *Journal of Catalysis* 146 (1): 292–305.

Yi, N., R. Si, H. Saltsburg, and M. Flytzani-Stephanopoulos. 2010a. "Active Gold Species on Cerium Oxide Nanoshapes for Methanol Steam Reforming and the Water Gas Shift Reactions." *Energy & Environmental Science* 3 (6): 831–7.

Yi, N., R. Si, H. Saltsburg, and M. Flytzani-Stephanopoulos. 2010b. "Steam Reforming of Methanol over Ceria and Gold-Ceria Nanoshapes." *Applied Catalysis B: Environmental* 95 (1): 87–92.

Yu, X., J. He, D. Wang, Y. Hu, H. Tian, and Z. He. 2011. "Facile Controlled Synthesis of Pt/MnO_2 Nanostructured Catalysts and Their Catalytic Performance for Oxidative Decomposition of Formaldehyde." *The Journal of Physical Chemistry C* 116 (1): 851–60.

Yu, X., J. He, D. Wang, Y. Hu, H. Tian, T. Dong, and Z. He. 2013. "Preparation of Au 0.5 Pt 0.5/MnO_2/Cotton Catalysts for Decomposition of Formaldehyde." *Journal of Nanoparticle Research* 15 (8): 1832.

Yuan, J., P. Xu, J. Wang, W. Zhang, J. Zhou, A. Lai, and L. Wang. 2020. "Experimental Study on the Removal of Formaldehyde by Plasma-Catalyst." In *IOP Conference Series: Earth and Environmental Science*, vol. 435, no. 1, 012004.

Zang, L., W. Macyk, C. Lange, W. F. Maier, C. Antonius, D. Meissner, and H. Kisch. 2000. "Visible-light Detoxification and Charge Generation by Transition Metal Chloride Modified Titania." *Chemistry: A European Journal* 6 (2): 379–84.

Zazueta, A. L., H. Destaillats, and G. L. Puma. 2013. "Radiation Field Modeling and Optimization of a Compact and Modular Multi-Plate Photocatalytic Reactor (MPPR) for Air/water Purification by Monte Carlo Method." *Chemical Engineering Journal* 217: 475–85.

Zhai, Y., D. Pierre, R. Si, W. Deng, P. Ferrin, A. U. Nilekar, G. Peng, J. A. Herron, D. C. Bell, H. Saltsburg, and M. Mavrikakis. 2010. "Alkali-Stabilized Pt-OH_x Species Catalyze Low-Temperature Water–Gas Shift Reactions." *Science* 329 (5999): 1633–6.

Zhang, C. B., and H. He. 2005. "Elimination of Formaldehyde over Cu-Al_2O_3 Catalyst at Room Temperature." *Journal of Environmental Sciences* 17 (3): 429–32.

Zhang, C., and H. He. 2007. "A Comparative Study of TiO_2 Supported Noble Metal Catalysts for the Oxidation of Formaldehyde at Room Temperature." *Catalysis Today* 126 (3): 345–50.

Zhang, C., H. He, and K. I. Tanaka. 2005. "Perfect Catalytic Oxidation of Formaldehyde over a Pt/TiO_2 Catalyst at Room Temperature." *Catalysis Communications* 6 (3): 211–4.

Zhang, C., H. He, and K. I. Tanaka. 2006. "Catalytic Performance and Mechanism of a Pt/TiO_2 Catalyst for the Oxidation of Formaldehyde at Room Temperature." *Applied Catalysis B: Environmental* 65 (1): 37–43.

Zhang, Z., O. Bondarchuk, B. D. Kay, J. M. White, and Z. Dohnálek. 2007. "Direct Visualization of 2-Butanol Adsorption and Dissociation on TiO_2 (110)." *The Journal of Physical Chemistry C* 111 (7): 3021–7.

Zhang, C., F. Liu, Y. Zhai, H. Ariga, N. Yi, Y. Liu, K. Asakura, M. Flytzani-Stephanopoulos, and H. He. 2012. "Alkali-Metal-Promoted Pt/TiO_2 Opens a More Efficient Pathway to Formaldehyde Oxidation at Ambient Temperatures." *Angewandte Chemie International Edition* 51 (38): 9628–32.

Zhang, C., Y. Li, Y. Wang, and H. He. 2014. "Sodium-promoted Pd/TiO_2 for Catalytic Oxidation of Formaldehyde at Ambient Temperature." *Environmental Science & Technology* 48 (10): 5816–22.

Zhang, J., Y. Li, Y. Zhang, M. Chen, L. Wang, C. Zhang, and H. He. 2015a. "Effect of Support on the Activity of Ag-Based Catalysts for Formaldehyde Oxidation." *Scientific Reports* 5.

Zhang, S., X. S. Li, B. Zhu, J. L. Liu, X. Zhu, A. M. Zhu, and B. W. Jang. 2015b. "Atmospheric-Pressure O_2 Plasma Treatment of Au/TiO_2 Catalysts for CO Oxidation." *Catalysis Today* 256: 142–7.

Zhang, Z., Z. Jiang, and W. Shangguan. 2016. "Low-temperature Catalysis for VOCs Removal in Technology and Application: a State-of-the-Art Review." *Catalysis Today* 264: 270–8.

Zhang, S., M. Wang, Z. Lu, C. Ma, and W. Jia. 2019. "Biomass Bricks with Excellent Indoor Formaldehyde Capture and Transformation Performance." *ACS Sustainable Chemistry & Engineering* 7 (13): 11493–9.

Zhao, J., and X. Yang. 2003. "Photocatalytic Oxidation for Indoor Air Purification: a Literature Review." *Building and Environment* 38 (5): 645–54.

Zhao, W., W. Ma, C. Chen, J. Zhao, and Z. Shuai. 2004. "Efficient Degradation of Toxic Organic Pollutants with $Ni_2O_3/TiO_{2-x}B_x$ under Visible Irradiation." *Journal of the American Chemical Society* 126 (15): 4782–3.

Zhao, D. Z., C. Shi, X. S. Li, A. M. Zhu, and B. W. Jang. 2012. "Enhanced Effect of Water Vapor on Complete Oxidation of Formaldehyde in Air with Ozone over MnO_X Catalysts at Room Temperature." *Journal of Hazardous Materials* 239: 362–9.

Zhou, K., and Y. Li. 2012. "Catalysis Based on Nanocrystals with Well-Defined Facets." *Angewandte Chemie International Edition* 51 (3): 602–13.

Zhu, Z., and R. J. Wu. 2015. "The Degradation of Formaldehyde Using a Pt@ TiO_2 Nanoparticles in Presence of Visible Light Irradiation at Room Temperature." *Journal of the Taiwan Institute of Chemical Engineers* 50: 276–81.

Zhu, X., M. Shen, L. L. Lobban, and R. G. Mallinson. 2011. "Structural Effects of Na Promotion for High Water Gas Shift Activity on Pt–Na/TiO_2." *Journal of Catalysis* 278 (1): 123–32.

Zou, L., Y. Luo, M. Hooper, and E. Hu. 2006. "Removal of VOCs by Photocatalysis Process Using Adsorption Enhanced TiO_2–SiO_2 Catalyst." *Chemical Engineering and Processing: Process Intensification* 45 (11): 959–64.